Materials Chemistry and Physics 251 (2020) 123076

Contents lists available at ScienceDirect

Materials Chemistry and Physics

journal homepage: www.elsevier.com/locate/matchemphys

The influence of chitosan coating on the controlled release behaviour of zinc/aluminium-layered double hydroxide-quinclorac composite

Sharifah Norain Mohd Sharif [a], Norhayati Hashim [a,b,*], Illyas Md Isa [a,b], Suriani Abu Bakar [c], Mohamad Idris Saidin [a], Mohamad Syahrizal Ahmad [a], Mazidah Mamat [d], Mohd Zobir Hussein [e]

[a] Department of Chemistry, Faculty of Science and Mathematics, Universiti Pendidikan Sultan Idris, 35900, Tanjong Malim, Perak, Malaysia
[b] Nanotechnology Research Centre, Faculty of Science and Mathematics, Universiti Pendidikan Sultan Idris, 35900, Tanjong Malim, Perak, Malaysia
[c] Department of Physics, Faculty of Science and Mathematics, Universiti Pendidikan Sultan Idris, 35900, Tanjong Malim, Perak, Malaysia
[d] School of Fundamental Science, Universiti Malaysia Terengganu, 21030, Kuala Terengganu, Terengganu, Malaysia
[e] Materials Synthesis and Characterization Laboratory, Institute of Advanced Technology, Universiti Putra Malaysia, 43400, Serdang, Selangor, Malaysia

HIGHLIGHTS

- The novel Zn/Al-LDH-QC was coated with chitosan.
- Characterisation studies were executed using PXRD, FTIR, TGA and FESEM.
- The release media for the release study mimic the paddy cultivation environment.
- Reveal the potential of Zn/Al-LDH-QC and Zn/Al-LDH-QC-Chi as new materials for CRF.

GRAPHICAL ABSTRACT

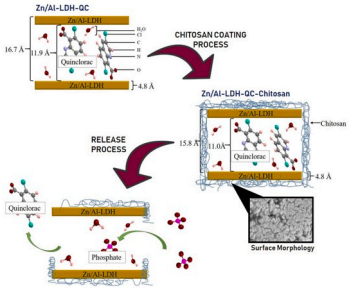

ARTICLE INFO

Keywords:
Zinc/aluminium-layered double hydroxide-quinclorac
Chitosan
Composite
Controlled release formulation
Kinetic

ABSTRACT

Controlled release formulations of herbicides have been recognised to have potential in reducing the adverse effects of conventional herbicides on our environment. In this work, the controlled release behaviour of quinclorac (QC) from zinc/aluminium-layered double hydroxide-quinclorac (Zn/Al-LDH-QC) and its chitosan-coated composite Zn/Al-LDH-QC-Chi into aqueous solutions of Na_3PO_4, Na_2SO_4 and NaCl were studied. The physicochemical properties of both composites were studied initially, using powder X-ray diffraction (PXRD), Fourier transform infrared (FTIR), thermogravimetric and derivative thermogravimetric analysis (TGA/DTG) and field emission scanning electron microscopy (FESEM) instruments, so that the effect of chitosan coating on their functional groups, thermal stabilities and surface morphology could be observed thoroughly. The results from the release studies showed that the presence of chitosan as a coating enhances the electrostatic attraction between the positively charged amino groups on the backbone of chitosan and the negatively charged QC anions, thus assisting in prolonging the time of release of QC. The kinetic studies revealed that both Zn/Al-LDH-QC and Zn/Al-LDH-QC-Chi composites obey second-order mechanisms, thus signifying that the release of QC into the release media by both composites took place via dissolution and ion exchange. These results therefore indicate the promising potential of Zn/Al-LDH-QC and Zn/Al-LDH-QC-Chi to overcome the drawbacks of the over-use of herbicides in paddy cultivation areas.

* Corresponding author. Department of Chemistry, Faculty of Science and Mathematics, Universiti Pendidikan Sultan Idris, 35900, Tanjong Malim, Perak, Malaysia.
E-mail address: norhayati.hashim@fsmt.upsi.edu.my (N. Hashim).

https://doi.org/10.1016/j.matchemphys.2020.123076
Received 6 December 2018; Received in revised form 13 December 2019; Accepted 12 April 2020
Available online 17 April 2020

1. Introduction

The use of pesticides in the agriculture sector is essential so as to increase the productivity of the harvested yield [1]. However, the continuous application of pesticides may result in numerous bad effects on nature, such as air quality degradation, pollution of water bodies and extinction of threatened species [2–11]. Hence, controlled released formulation (CRF) was introduced as a new approach to alleviate the environmental issues triggered by pesticide residues and correspondingly improve the effectiveness of the pesticides [12–19].

CRF has attract great interest in recent years and has been exploited in various agrochemical fields. It has been implemented with several agrochemical agents, including fertilisers, plant growth enhancers and pesticides [20–25]. CRF has been proven to enhance weed management by increasing the prolonged time of release of active ingredients in pesticides and minimising ecological contamination caused by pesticides by permitting lower and constant concentrations of pesticides in the surroundings [26]. Therefore, pest problems can be diminished without polluting the environment or risking the health of pesticide operatives.

Coating is one of the essential procedures in the fabrication of controlled release agricultural formulations. This procedure entraps active agents inside another substance (wall material), which is designed to shield the interior material from unfavourable environmental conditions such as excessive moisture, light and oxygen, and subsequently to enhance the shelf-life of the coated materials and enable the slow delivery of the product through controlled diffusion processes [27]. This, therefore, results in minimal losses of the active ingredient to the environment and prevents pollution.

The material used to coat the internal substance is commonly called the coater, membrane, shell, capsule, carrier material, external phase or matrix [28]. The selection of coating materials is made based on the consideration of several criteria, such as the limitations of the coating material, the quality offered by the coating material to the shielded substance, concentration of the coating material, stability necessities, mode of delivery and cost restrictions [29].

The coating of pesticides may enhance the controlled released behaviour, enable targeted delivery, improve pesticide efficiency and restrain the unintentional spread of pesticide residues to the environment [13–18,30]. Many polysaccharide nanoparticles have been explored for coating purposes, and one of the most widely used is chitosan [25,31–36]. Chitosan is a linear biopolymer which consists of the monomers of 2-amino-2-deoxy-β-d-glucan with glycosidic linkages. Three types of reactive functional group are bonded to the chitosan structure: amino groups and both primary and secondary hydroxyl groups [37]. The chemical structure of chitosan is shown in Fig. 1. Chitosan is derived through the partial deacetylation of chitin, originated from shells of marine organisms such as shrimps and crabs [38]. Owing to its good biocompatibility, non-toxic nature, antifungal activity and excellent biodegradability, chitosan has become a type of cationic polysaccharide that is commonly exploited for pesticide coating purposes [39].

Quinclorac (QC), a type of herbicide extensively used in paddy cultivation has been successfully intercalated into the interlayer gallery of zinc/aluminium-layered double hydroxide (Zn/Al-LDH), as reported in our previous paper [40]. The Zn/Al-LDH-QC was synthesised using a co-precipitation method, with a Zn/Al molar ratio of 3.0:1.0. In this paper we aim to explore further the possibility of using the composite in CRF applications. Hence, the controlled release behaviour of Zn/Al-LDH-QC was studied in several salt solutions, including in sodium phosphate (Na_3PO_4), sodium sulphate (Na_2SO_4) and sodium chloride (NaCl). Zn/Al-LDH-QC coated with chitosan (Zn/Al-LDH-QC-Chi) composite was also synthesised in order to determine the impact of using chitosan as a coating material in enhancing CRF properties. Several techniques, including powder X-ray diffraction (PXRD), Fourier transform infrared (FTIR), thermogravimetric and derivative thermogravimetric analysis (TGA/DTG) and field emission scanning electron microscopy (FESEM) were used for characterisation purposes, to analyse the physicochemical properties of both Zn/Al-LDH-QC and Zn/Al-LDH-QC-Chi composites.

2. Experimental section

2.1. Reagents

$Zn(NO_3)_2{\cdot}6H_2O$ and $Al(NO_3)_3{\cdot}9H_2O$ were obtained from Systerm (Malaysia), both with purity of 98%. The intercalated guest ions, QC, was purchased from Essense (China) with 95% purity and the coating material, chitosan, was obtained from Sigma Aldrich (USA). The acetic acid used to dissolve the chitosan was obtained from HmbG Chemicals (Germany). The salt used to prepare the release media, sodium phosphate (Na_3PO_4) was purchased from Merck with 99.5% purity and the sodium sulphate (Na_2SO_4) and sodium chloride (NaCl) were obtained from Systerm (Malaysia), with 95.2% and 99.0% purity, respectively. All reagents used in the study were used as received without further purification, and all solutions used in this study were prepared using deionised water.

2.2. Synthesis of Zn/Al-LDH-QC and Zn/Al-LDH-QC chitosan-coated composite

The Zn/Al-LDH and Zn/Al-LDH-QC composite were synthesised using a co-precipitation method, under nitrogen atmosphere. Zinc nitrate and aluminium nitrate were used as precursors, with a Zn/Al molar ratio of 3.0:1.0. The method of synthesising the Zn/Al-LDH-QC composite was reported thoroughly in our recent paper [40].

The Zn/Al-LDH-QC-Chi composite was then synthesised by coating the Zn/Al-LDH composite with chitosan with mass ratio of 1.0:1.0. The coating procedure was initiated by dissolving 0.1 g of chitosan in 1% acetic acid, and 50 mL of deionised water was then added into the mixture. The chitosan solution was stirred at room temperature and left for 24 h, to dissolve the chitosan completely. Zn/Al-LDH-QC composite (0.1 g) was added to the chitosan solution and stirred for 18 h at room temperature. The mixture was centrifuged at 4000 rpm for 5 min and dried in oven at 60 °C for 24 h. The dried sample was ground and stored in a sample bottle for characterisation and controlled release study. Similar procedure was repeated on the Zn/Al-LDH, and the product was labelled as Zn/Al-LDH-Chi.

2.3. Characterisation of Zn/Al-LDH-QC and Zn/Al-LDH-QC chitosan-coated composite

The PXRD patterns of the samples were obtained using a PANalytical X-pert Pro MPD diffractometer in the range of 2–60° under the following condition; 30 mA, 40 kV, step size: 0.0330°, scan step time: 19.4434 s, using Co K-alpha radiation (0.15406 nm). The Fourier transform infrared (FTIR) spectra were recorded using a Nicolet FTIR spectrometer at 400–4000 cm^{-1}, with nominal resolution of 4 cm^{-1} and KBr disc technique. The TGA/DTG analysis was carried out using PerkinElmer Pyris 1 TGA thermo balance. The samples were heated from 35 to 1000 °C, with heating rate of 10 °C min^{-1} under nitrogen atmosphere. The surface morphology and the surface properties of the samples were

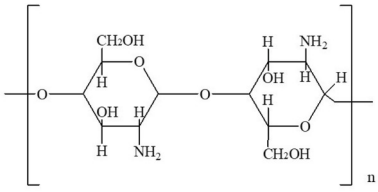

Fig. 1. The chemical structure of chitosan.

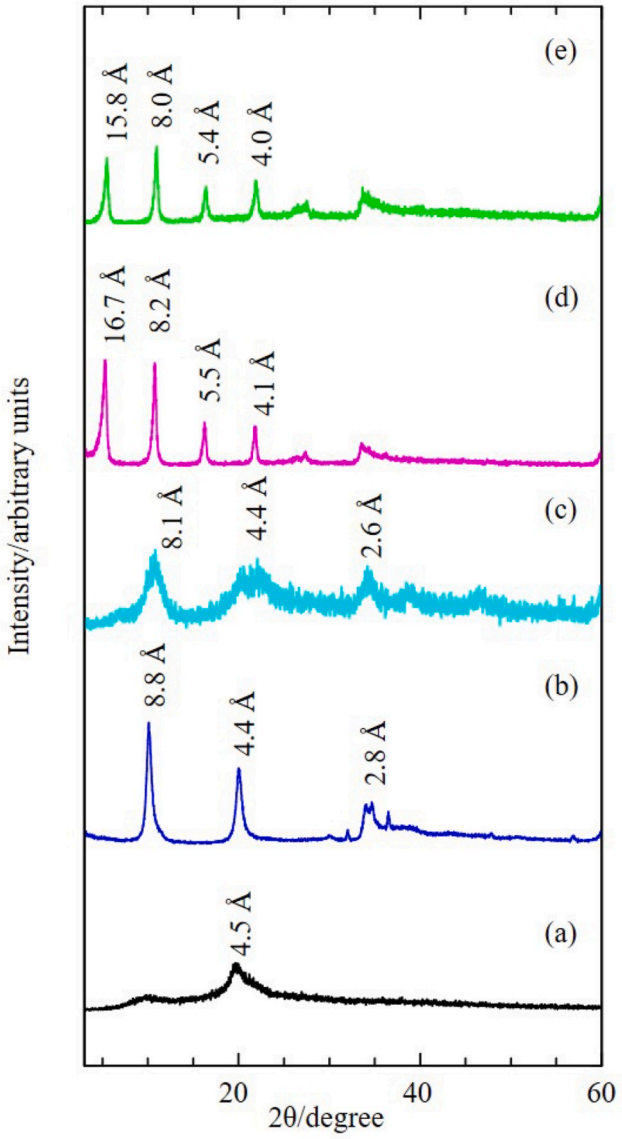

Fig. 2. PXRD patterns of (a) chitosan, (b) Zn/Al-LDH [40], (c) Zn/Al-LDH-Chi, (d) Zn/Al-LDH-QC [40], and (e) Zn/Al-LDH-QC-Chi.

analysed by FESEM (Hitachi SU 8020 UHR).

2.4. Controlled release formulation study of Zn/Al-LDH-QC and Zn/Al-LDH-QC chitosan-coated composite

The controlled released study of the Zn/Al-LDH-QC and Zn/Al-LDH-QC-Chi composites were conducted using a PerkinElmer UV–vis spectrometer. Deionised water was used as a blank and three types of salt solution, Na_3PO_4, Na_2SO_4 and NaCl, were used as release media. The aqueous solutions for the single system were prepared in 0.3 M, 0.5 M and 1.0 M whereas the binary and ternary system were prepared in 1.0 M aqueous solutions of several combination (PO_4^{3-}–SO_4^{2-}, PO_4^{3-}–Cl^- and SO_4^{2-}–Cl^- and PO_4^{3-}–SO_4^{2-}–Cl^-). Salt solution (3.5 mL) was placed in a cuvette and 0.6 mg of composite was then added. The cuvette was closed and covered with parafilm. The cuvette was left for a few days in the UV–vis spectrometer so that the controlled release behaviour could be observed. Study of the release from the composite was conducted using similar experimental conditions of UV–vis measurement (lambda max = 238.1 nm, time interval = 60 s, slit width = 1.0 nm, lamp change = 326.0 nm, ordinate max = 1.0 and ordinate min = 0.0).

3. Results and discussion

3.1. PXRD analysis

The PXRD patterns obtained from the analysis are shown in Fig. 2. In the PXRD pattern of Zn/Al-LDH, three obvious diffraction peaks can be observed, with basal spacings of 8.8, 4.4 and 2.8 Å [40]. Three peaks with almost similar basal spacing can also be observed in the PXRD pattern of the Zn/Al-LDH coated with chitosan (Zn/Al-LDH-Chi), with basal spacings of 8.1, 4.4 and 2.6 Å. The results obtained from PXRD analysis therefore reveal that the diffraction peaks of Zn/Al-LDH and the Zn/Al-LDH-QC, before and after coating with chitosan, were not very different from one another. The presence of the nitrate peak in the PXRD pattern of Zn/Al-LDH (8.8 Å) and Zn/Al-LDH-Chi (8.1 Å), indicates that nitrate ions remained as the counter-ions in both samples. Nevertheless, obvious changes in terms of crystallinity can be seen in the PXRD pattern of Zn/Al-LDH after undergoing the coating process. The PXRD diffraction peaks of Zn/Al-LDH-Chi are broader and of lower intensity compared to those of Zn/Al-LDH, hence reflecting the disordered layered structure of Zn/Al-LDH-Chi due to the influence of the amorphous structure of the chitosan [41].

Four diffraction peaks can be seen in the PXRD patterns of both Zn/Al-LDH-QC and Zn/Al-LDH-QC-Chi, with basal spacings of 16.7, 8.2, 5.5 and 4.1 Å in Zn/Al-LDH-QC and 15.8, 8.0, 5.4 and 4.0 Å in Zn/Al-LDH-QC-Chi. Similar to the trend of the coated and uncoated Zn/Al-LDH, the basal spacing values of Zn/Al-LDH-QC and Zn/Al-LDH-QC-Chi were generally similar. Even though both Zn/Al-LDH-QC and Zn/Al-LDH-QC-Chi demonstrate the appearance of intense, sharp and symmetrical diffraction peaks, the intensities of the diffraction peaks in the PXRD pattern of Zn/Al-LDH-QC-Chi are slightly lower compared to those of Zn/Al-LDH-QC. This, therefore, indicates that the crystallinity of Zn/Al-LDH-QC-Chi is reduced due to the amorphous characteristic of the chitosan [41]. The intercalation peaks that validate the presence of QC in the interlayer gallery of both samples appeared at low 2θ angles (basal spacings of 16.7 and 15.8 Å), which can be seen in both PXRD patterns [40]. Therefore, the minor changes in the basal spacing values between the uncoated and the chitosan-coated samples prove that the type of ion intercalated in the interlayer gallery of the Zn/Al-LDH was barely affected by the coating process.

3.2. Spatial arrangement of chitosan coated Zn/Al-LDH-QC composite

The QC anion was proposed to be oriented in the interlayer gallery of Zn/Al-LDH in a monolayer arrangement, as reported in our previous paper [40]. The QC anion was held in that orientation by the electrostatic attraction that exists between the carboxylate group of QC and the positively charged layer of Zn/Al-LDH. The arrangement was predicted using Chem 3D Ultra 8.0 software after considering the basal spacing of the Zn/Al-LDH-QC composite obtained from the PXRD analysis (16.7 Å), the thickness of the Zn/Al-LDH layer (4.8 Å), and the three-dimensional molecular structure of QC (length, height and thickness of QC were determined to be 11.8, 9.2 and 4.1 Å, respectively) [40,42].

As mentioned in the previous section, the PXRD pattern of the samples, before and after the coating process, are not very different from one another. Although the basal spacing values are similar, the values were slightly changed after the composite was coated. It was revealed that there was a reduction on the basal spacing of the Zn/Al-LDH-QC, from 16.7 Å to 15.8 Å, thus decreasing the height of the interlayer gallery from 11.9 Å to 11.0 Å. The reduction can be elucidated based on the interactions between the hydroxyl groups on the surface of Zn/Al-LDH and the chitosan via hydrogen bonding and coordinate covalent bond formation, hence causing the shrinking of the composite after the coating process [43]. The changes signify that even though the QC was still intercalated in the interlayer gallery of the Zn/Al-LDH-QC composite, the coating process caused a minor alteration in the spatial orientation of QC. The reduction of the interlayer gallery height

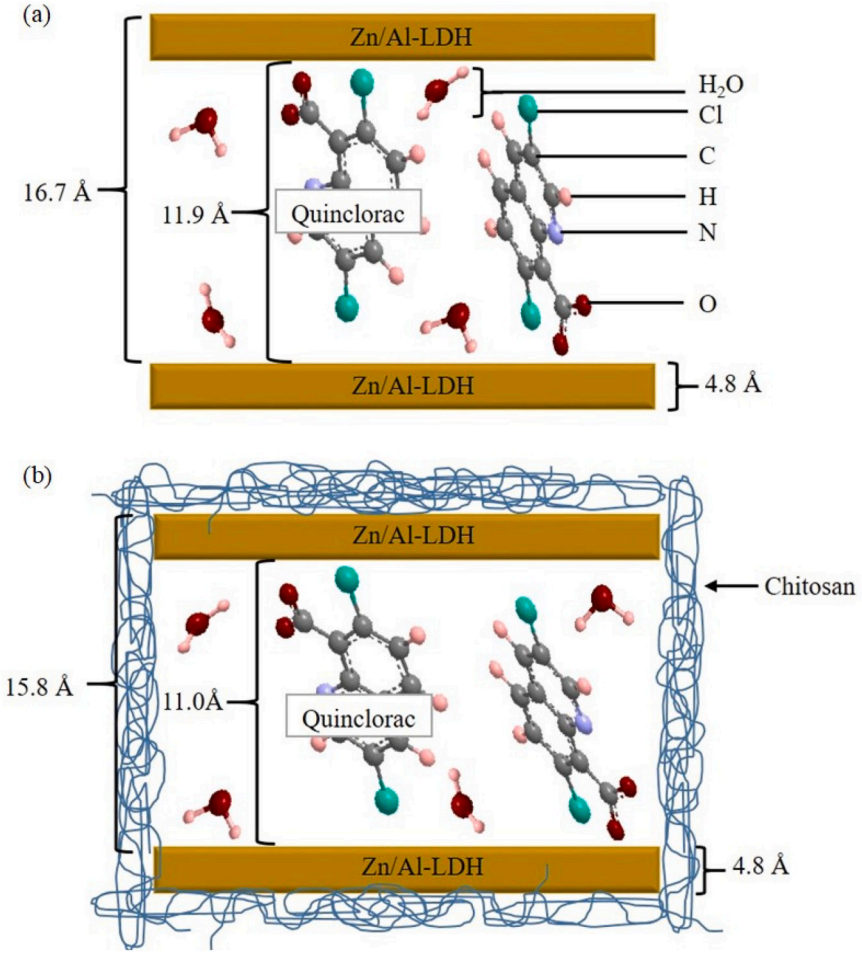

Fig. 3. Spatial arrangement of QC in the interlayer gallery of Zn/Al-LDH (a) before coating with chitosan and (b) after coating with chitosan.

triggered the QC anions to arrange themselves in a more tilted position, while preserving the orientation of the monolayer arrangement. The predicted spatial arrangement of QC in the interlayer gallery of Zn/Al-LDH before and after the composite was coated with chitosan is illustrated in Fig. 3.

3.3. FTIR analysis

Fig. 4 shows the FTIR spectra of (a) host Zn/Al-LDH, (b) QC anion, (c) Zn/Al-LDH-QC composite, (d) chitosan, (e) chitosan coated Zn/Al-LDH (Zn/Al-LDH-Chi), and (f) Zn/Al-LDH-QC-Chi composite. By comparing the peaks appearing in each spectrum, the changes in the functional groups after chitosan coating can be observed.

The FTIR spectra of chitosan shows several typical peaks, at 3497 cm^{-1} (O–H stretching), 1665 cm^{-1} (amide C–O stretching), 1556 cm^{-1} (amide N–H bending and C–N stretching) and 1052 cm^{-1} (C–O–C stretching) [40,43–45]. Similar peaks can be observed in the FTIR spectra of Zn/Al-LDH-Chi at 3345, 1645, 1547 and 1036 cm^{-1}, respectively. The characteristic peaks of Zn/Al-LDH can also be seen in the FTIR spectra of Zn/Al-LDH-Chi at 1371 cm^{-1} (originally found in the FTIR spectra of Zn/Al-LDH at 1385 cm^{-1}), 567 cm^{-1} (originally found in the FTIR spectra of Zn/Al-LDH at 604 cm^{-1}) and 444 cm^{-1} (originally found in the FTIR spectra of Zn/Al-LDH at 430 cm^{-1}), corresponding to the symmetric stretching of NO_3^-, the bending vibration of Al–OH and the bending vibration of Zn–Al–OH, respectively [40,46].

Comparison of the FTIR spectra also reveals that the peaks present in the spectrum of the coated Zn/Al-LDH-QC-Chi composite are mostly similar to those of Zn/Al-LDH-QC. A broad and obvious absorption peak found in the FTIR spectrum of the coated Zn/Al-LDH-QC-Chi at 3330 cm^{-1}, which represents the OH groups found both in interlayer water and hydroxide basal layer, was also found in the spectra of Zn/Al-LDH and Zn/Al-LDH-QC at 3450 cm^{-1} and 3342 cm^{-1}, respectively [40,47]. The peak that represents the C–N stretching mode in an aromatic compound can be seen in the spectra of the coated Zn/Al-LDH-QC-Chi at 1367 cm^{-1} and of Zn/Al-LDH-QC at 1330 cm^{-1} [40]. The peak that corresponds to the stretching of C–O was found in the spectra both of the coated Zn/Al-LDH-QC-Chi and of Zn/Al-LDH-QC at 1098 cm^{-1} and 1092 cm^{-1}, respectively. The peaks that signify the stretching mode of the carboxylate anion of the coated Zn/Al-LDH-QC-Chi were seen at 1480 cm^{-1} and 1568 cm^{-1}, whereas for Zn/Al-LDH-QC similar peaks were seen at 1473 cm^{-1} and 1564 cm^{-1} [40,48]. The bending vibrations of Al–OH and Zn–Al–OH are also present in the spectra both of the coated Zn/Al-LDH-QC-Chi at 558 cm^{-1} and 425 cm^{-1}, and of Zn/Al-LDH-QC at 456 cm^{-1} and 512 cm^{-1}, respectively [23]. Similar peaks that appeared in the spectra of both Zn/Al-LDH-QC and Zn/Al-LDH-QC-Chi composites show that the functional groups of Zn/Al-LDH-QC were unaffected after the composite was coated with chitosan, hence indicating that no modification or interaction occurred between the chitosan and Zn/Al-LDH-QC, and the QC remained intercalated in the interlayer gallery of Zn/Al-LDH in both coated and uncoated composites [45]. The FTIR analysis showed good agreement with the results obtained from PXRD analysis, as the PXRD pattern remained the same after the composite was coated, although the peak positions were slightly shifted.

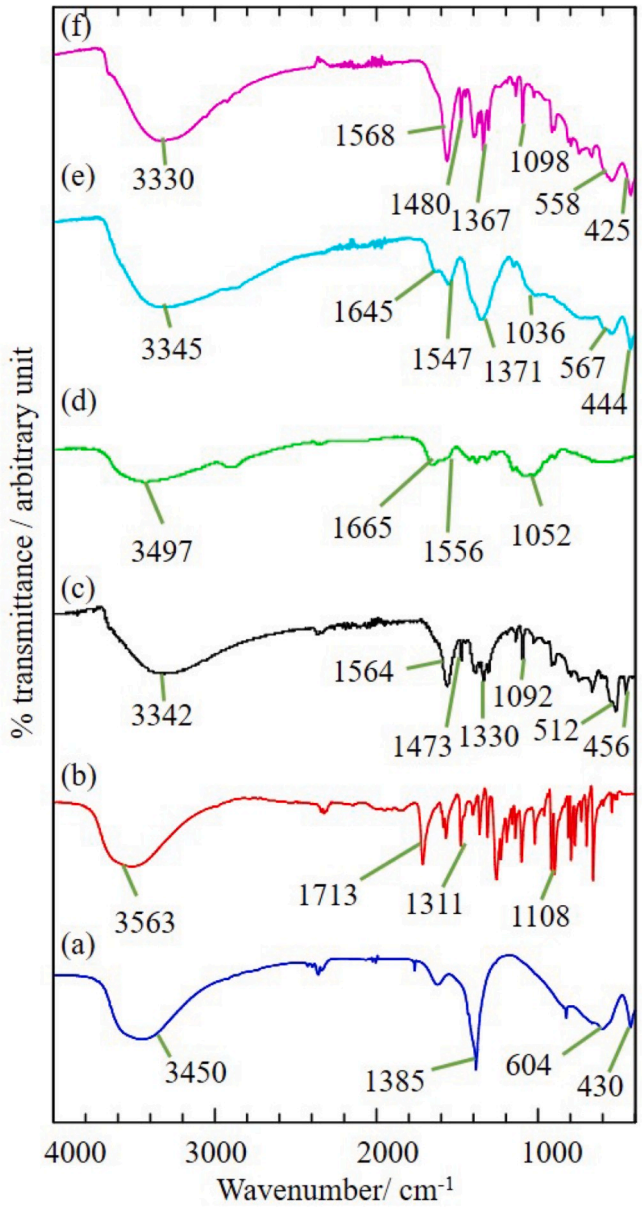

Fig. 4. FTIR spectra of (a) Zn/Al-LDH [40], (b) QC anion [40], (c) Zn/Al-LDH-QC [40], (d) chitosan, (e) Zn/Al-LDH-Chi, and (f) Zn/Al-LDH-QC-Chi.

3.4. Thermal stability studies

The results obtained from the TGA/DTG thermal studies of chitosan, Zn/Al-LDH-Chi and Zn/Al-LDH-QC-Chi are shown in Fig. 5. The value of maximum thermal decomposition (T_{max}) of each peak in the TGA/DTG curve and its percentage decomposition were compare with the result obtained in the previous paper, so that the influence of chitosan coating on the thermal behaviour of Zn/Al-LDH and Zn/Al-LDH-QC can be observed [40]. The comparison was summarised in Table 1.

The TGA/DTG curve generally demonstrate that each sample seems to have a distinct thermal decomposition pattern. The decomposition of the Zn/Al-LDH host occurred in three stages as it was heated from 35 to 1000 °C. The decomposition is due to the elimination of the water from the outer surface (121.8 °C), the removal of interlayer water molecules (251.5 °C) and the dihydroxylation of Zn/Al-LDH (331.0 °C) [49]. The Zn/Al-LDH host was also coated with chitosan to observe the effect of coating on its thermal decomposition. Zn/Al-LDH-Chi decomposes in three stages, at 71.2, 238.4 and 953.1 °C. The TGA/DTG results

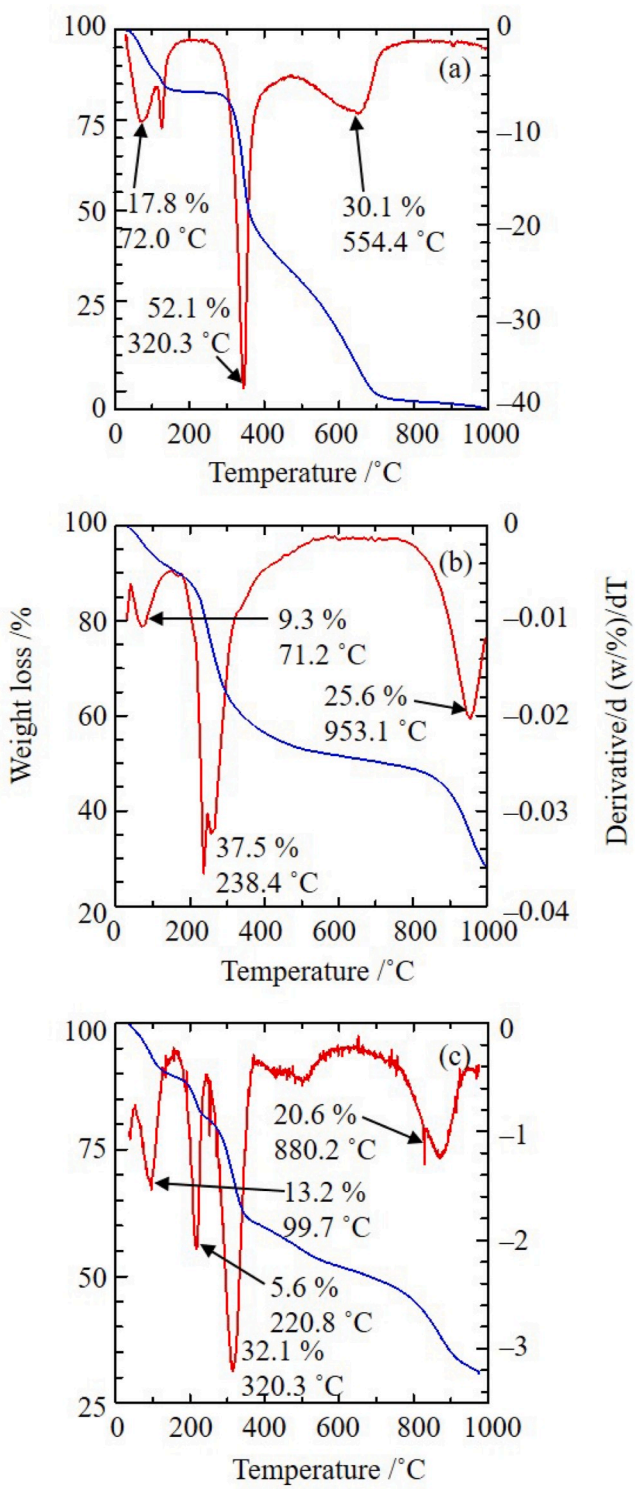

Fig. 5. TGA/DTG curves of (a) chitosan, (b) Zn/Al–LDH–Chi and (c) Zn/Al–LDH–QC–Chi.

therefore reveal that the maximum temperature of the Zn/Al-LDH-Chi (953.1 °C) was found to be higher compared to the pristine Zn/Al-LDH host (331.0 °C).

A similar trend was also observed when the Zn/Al-LDH-QC composite was coated with chitosan. The thermal studies show that the uncoated Zn/Al-LDH-QC composite decomposes in three stages, at 97.7, 223.5 and 321.7 °C. The first two decomposition stages are comparable to the thermal decomposition of Zn/Al-LDH, owing to the elimination of

Table 1
TGA/DTG data of weight loss for chitosan, Zn/Al-LDH, Zn/Al-LDH-Chi, Zn/Al-LDH-QC and Zn/Al-LDH-QC-Chi.

Thermal decomposition		Samples				
		Chitosan	Zn/Al-LDH	Zn/Al-LDH-Chi	Zn/Al-LDH-QC	Zn/Al-LDH-QC-Chi
Stage 1	T_{max} (°C)	72.0	121.8	71.2	97.7	99.7
	Percentage (%)	17.8	5.5	9.3	9.8	13.2
Stage 2	T_{max} (°C)	320.3	251.5	238.4	223.5	220.8
	Percentage (%)	52.1	15.3	37.5	9.2	5.6
Stage 3	T_{max} (°C)	554.4	331.0	953.1	321.7	320.3
	Percentage (%)	30.1	8.6	25.6	22.5	32.1
Stage 4	T_{max} (°C)	–	–	–	–	880.2
	Percentage (%)	–	–	–	–	20.6
Ref.		Present paper	[40]	Present paper	[40]	Present paper

the outer surface and interlayer water molecules, respectively. The third decomposition is due to combustion of the organic moiety that was loaded in the interlayer gallery of the Zn/Al-LDH-QC composite [40]. However, the thermal decomposition of Zn/Al-LDH-QC-Chi was seen to happen in four stages. The first three decomposition stages took place at temperatures not greatly different from the decomposition of Zn/Al-LDH-QC (99.7, 220.8 and 320.3 °C), whereas the last decomposition stage took place at a significantly high temperature: 880.2 °C. The maximum temperature of the Zn/Al-LDH-QC-Chi composite (880.2 °C) was determined to be higher compared than that of the Zn/Al-LDH-QC composite (312.7 °C), indicating that the chitosan coating does confer better thermal stability on the synthesised composite.

3.5. Surface morphology analysis

The morphological characteristics of the pure chitosan, Zn/Al-LDH, Zn/Al-LDH-Chi, Zn/Al-LDH-QC and Zn/Al-LDH-QC-Chi were analysed by FESEM, and the images obtained are shown in Fig. 6. Obvious transformations can be seen when comparing the surface morphology of the uncoated samples with the chitosan-coated samples. Although both uncoated and coated Zn/Al-LDH possess typical agglomerated, irregular and non-porous plate-like structures, the surface textures of both samples are quite different. The presence of chitosan as a coating material seems to flatten out the surface of the Zn/Al-LDH-Chi, resulting in the surface of Zn/Al-LDH-Chi to be more even than its uncoated form. As for

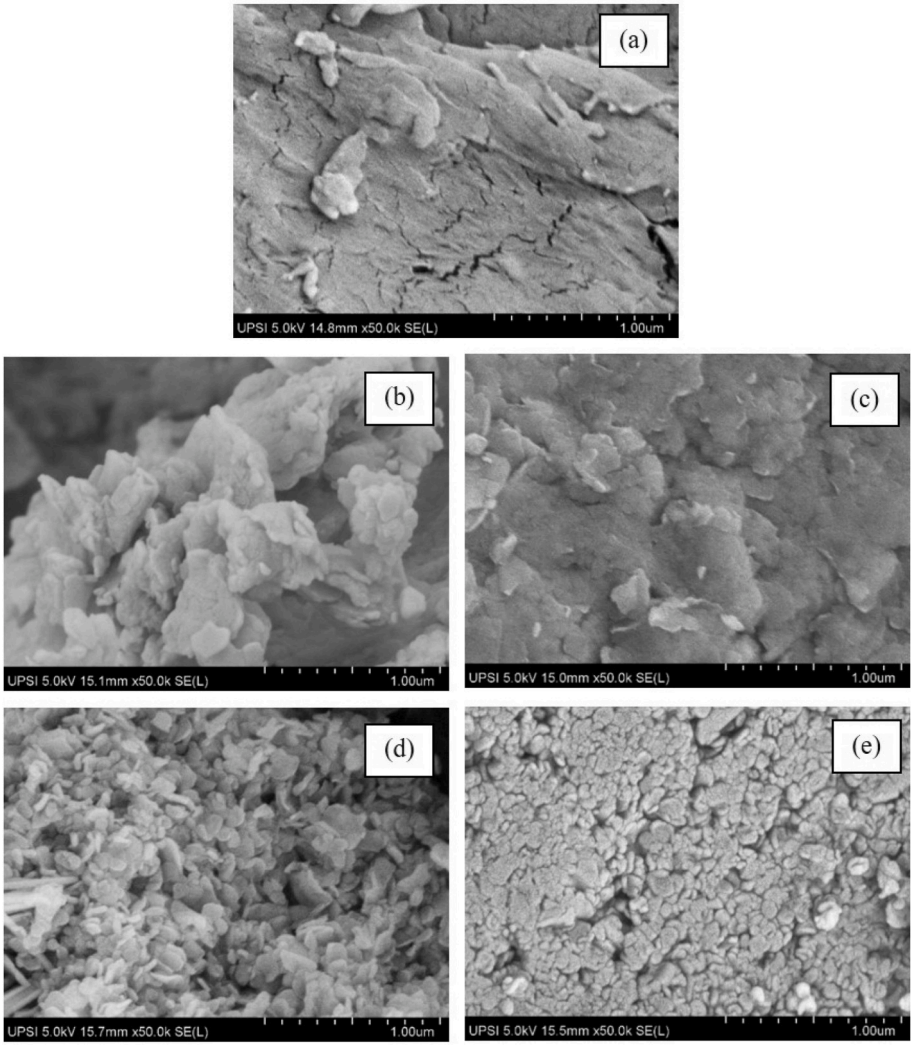

Fig. 6. Surface morphology of (a) chitosan, (b) Zn/Al-LDH, (c) Zn/Al-LDH-Chi, (d) Zn/Al-LDH-QC, and (e) Zn/Al-LDH-QC-Chi.

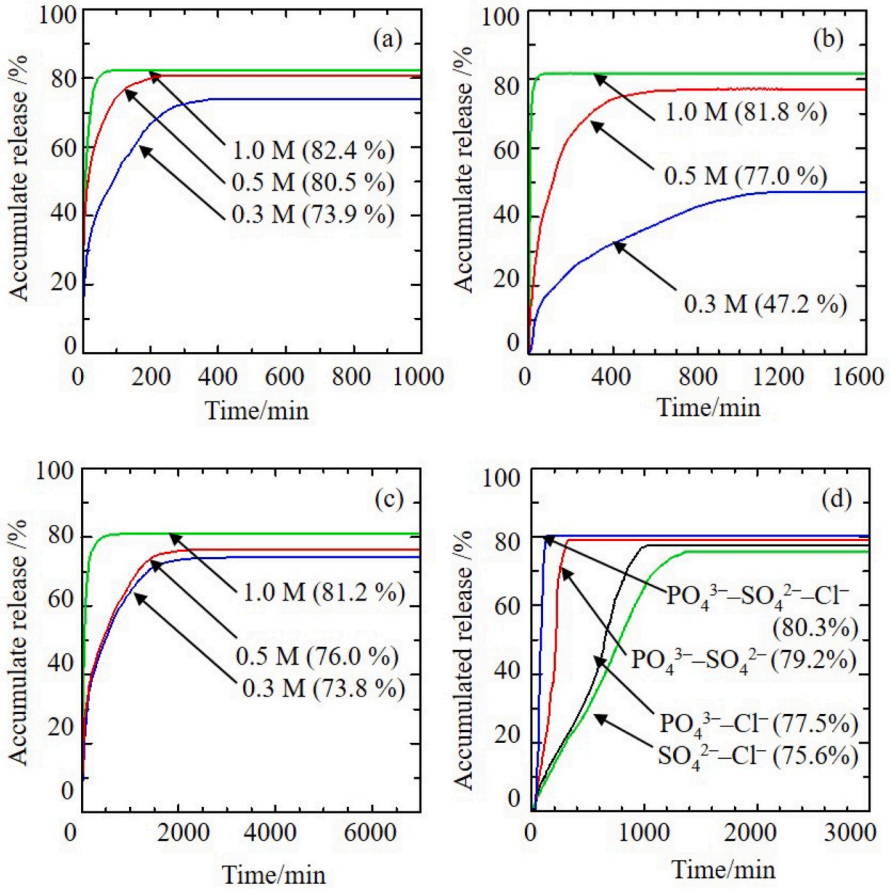

Fig. 7. Release profiles of QC from Zn/Al–LDH–QC into aqueous solutions of (a) sodium phosphate, (b) sodium sulphate, (c) sodium chloride and (d) phosphate, sulphate and chloride mixture.

Zn/Al-LDH-QC, the uncoated composite shows a tiny plate-like structure, with non-uniform particle size and shape [40]. The coating process causes the Zn/Al-LDH-QC-Chi composite to compress its surface; thus becoming flatter and more compact, while preserving its tiny plate-like structure. Therefore, it can be deduced from the surface morphology analysis that the presence of chitosan as coating material leads to some morphological modifications to both Zn/Al-LDH and Zn/Al-LDH-QC composites.

3.6. Study of release from Zn/Al-LDH-QC composite into various aqueous solutions

The anion exchange ability of Zn/Al–LDH allows the anion exchange process to take place between the intercalated QC anions and the anions present in the aqueous solutions [50]. The higher affinity, smaller size and higher charge density possessed by the anions in the aqueous solution, as compared to those intercalated into the layered hydroxide host material, are the main factors that lead to the anion exchange process, and which subsequently affect the release behaviour of the intercalated anions [51–53].

The QC is normally used to eliminate the weeds that invade the paddy cultivation area and disrupt the paddy growth, whereas the PO_4^{3-}, SO_4^{2-} and Cl^- are the type of anions that can actually be found in the soil of areas for paddy cultivation. Hence, these aqueous solutions of Na_3PO_4, Na_2SO_4, and NaCl were selected as the release media in the study due to their ability to provide the required anions. The release profiles of Zn/Al–LDH–QC into single, binary and ternary systems of Na_3PO_4, Na_2SO_4 and NaCl aqueous solutions are shown in Fig. 7. In the single system, each aqueous solutions were prepared at three concentrations (0.3 M, 0.5 M and 1.0 M) and as for the binary and ternary system, the mixtures were prepared in 1.0 M.

The release profile reveals that the release of QC into the aqueous solution is greatly dependent on the type of anion present in the aqueous solution. In the single system, the accumulated percentage release was dominated by PO_4^{3-}, in the order $PO_4^{3-} > SO_4^{2-} > Cl^-$, with maximum percentage releases of 82.4, 81.8 and 81.2%, respectively. Higher amounts of QC were released when exposed to the Na_3PO_4 solution, due to the fact that the PO_4^{3-} has a higher charge density than the other two anions, therefore strengthening its ion–exchange ability [42]. The release of QC from the Zn/Al–LDH–QC composite is also directly related to the concentration of the salt solutions, as can be seen from the release profile, where the percentage release of QC is generally increased with increases in salt concentration. The increase is triggered by the large number of salt ions that are present in salt solutions at higher concentrations, which thereby permit more ion exchange to be achieved between the interlayer QC and the salt ions in the aqueous solutions [48].

The time taken for the release of QC from the Zn/Al–LDH–QC composite to reach equilibrium was found to vary with each aqueous solution, in the order $Cl^- > SO_4^{2-} > PO_4^{3-}$, and the release rate also increased with increasing salt concentration. In the release of QC from the Zn/Al–LDH–QC composite into the 0.3 M, 0.5 M and 1.0 M of Na_3PO_4 solutions, fast release of QC can be seen in the first 0–356, 0–221 and 0–99 min, respectively, followed by slower release, before the release equilibrium is reached. In the Na_2SO_4 solution, the fast release occurred in the first 0–1161 min (0.3 M), 0–714 min (0.5 M) and 0–84 min (1.0 M), whereas in the NaCl solution, the fast release occurred in the first 0–2639 min (0.3 M), 0–2168 min (0.5 M) and 0–693 min (1.0 M). Hence, based on the results obtained from the release study, the

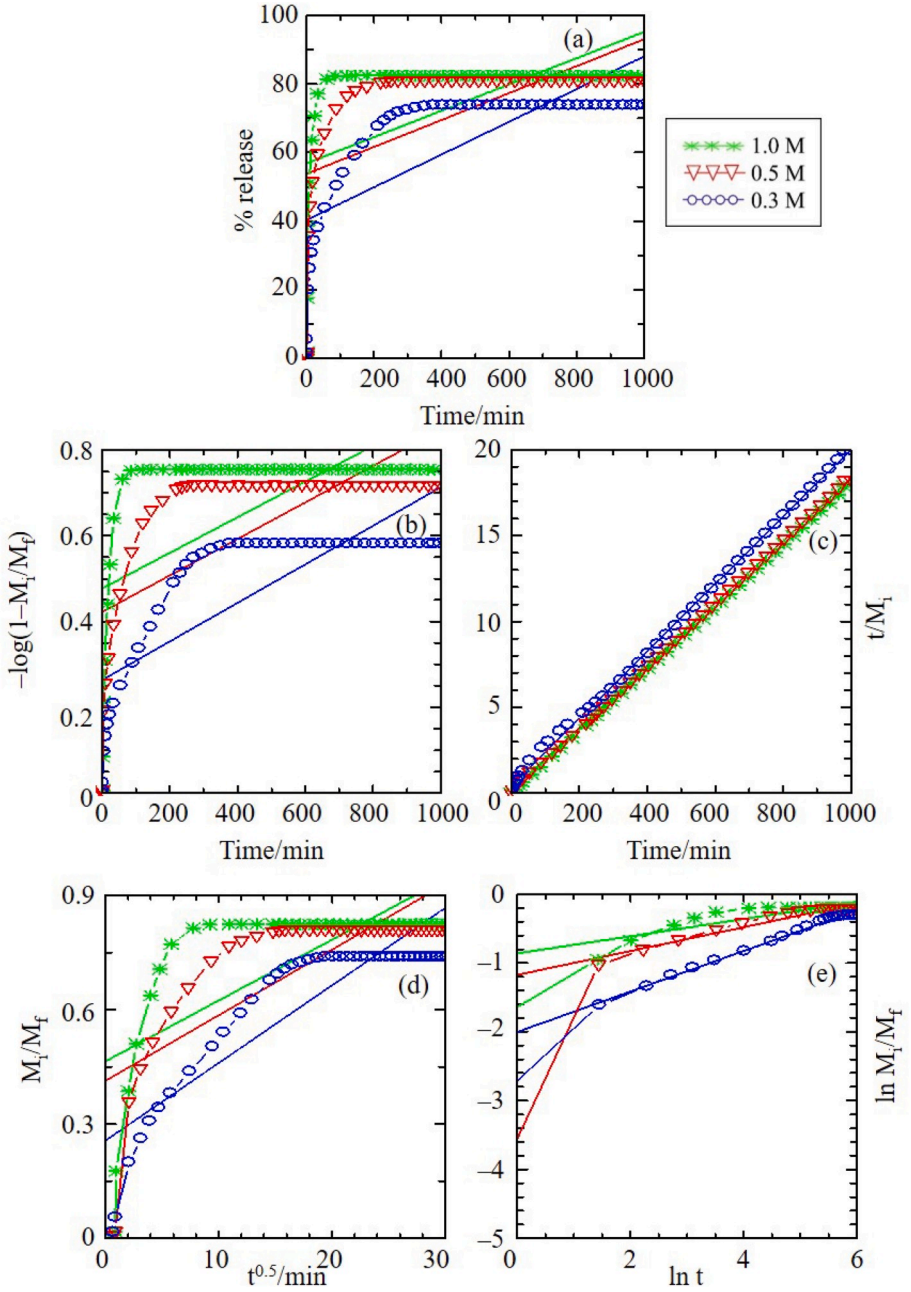

Fig. 8. Fitting of the data for QC release from Zn/Al-LDH-QC composite into sodium phosphate solution for the (a) zero order, (b) first-order, (c) pseudo second order, (d) parabolic diffusion and (e) Fickian diffusion models.

slowest release took place in the NaCl solution. The monovalent nature of the Cl^- ions causing them to have a lower affinity towards the positively charged layer of Zn/Al–LDH, compared to the trivalent PO_4^{3-} and divalent SO_4^{2-} ions; hence slowing the release from the Zn/Al–LDH–QC. The slow release of QC into NaCl solution compared to the other release media used in this study seems to be in good agreement with recent studies [42,48,54].

As for the release of QC from the Zn/Al–LDH–QC composite in binary release media, the highest percentage of accumulated release was observed when the release process was conducted in the aqueous solution containing PO_4^{3-} and SO_4^{2-} anions (79.2%), followed by release in the aqueous solution containing PO_4^{3-} and Cl^- anions (77.5%) and finally the aqueous solution containing SO_4^{2-} and Cl^- anions (75.6%). The time releases of QC in the release media were found to be 329, 1015 and 1359 min, respectively. These results demonstrate that the presence of PO_4^{3-} led to an acceleration in the release process, whereas the presence of Cl^- assisted in slowing the release process. This release behaviour can be related to the charge density of the PO_4^{3-} and Cl^- anions. The phosphate undergoes multiple hydrolysis processes, leaving the tertiary PO_4^{3-} left in the release media [55]. The higher charge density of the PO_4^{3-} anions compare to the SO_4^{2-} and Cl^- anions make it easier for the PO_4^{3-} anions to be attracted to the positively charge Zn/Al–LDH layer, hence causing the release rate in the release media containing PO_4^{3-} anions to be faster. In the ternary release media containing all three anions, PO_4^{3-}, SO_4^{2-} and Cl^-, 80.3% of intercalated QC was found to be released into the release media, within 138 min, which was the fastest release process with the highest accumulated release amongst the release media containing multiple type of anions.

Based on the results obtained in the release study of Zn/Al–LDH–QC using the release media of single, binary and ternary systems, it can be

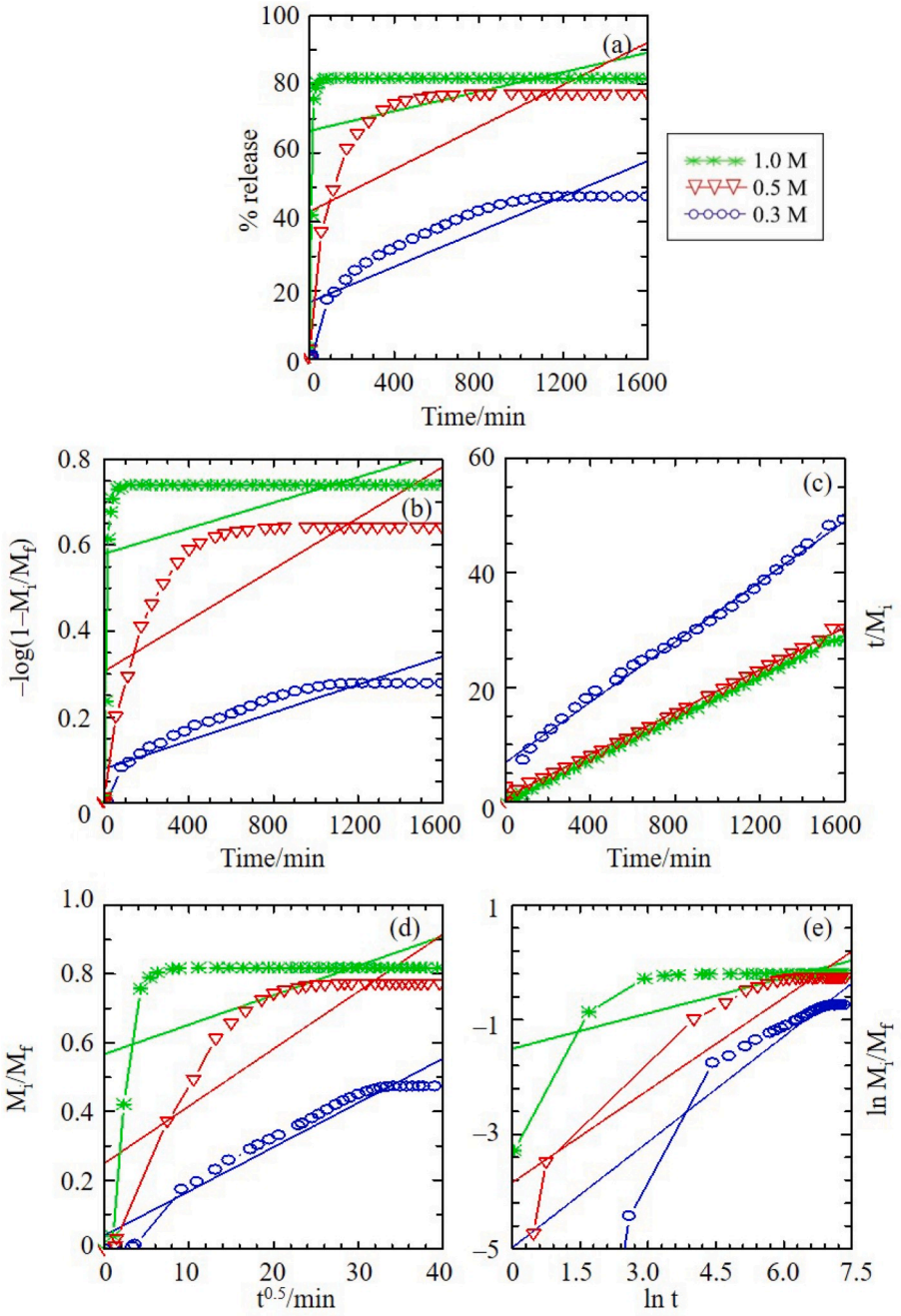

Fig. 9. Fitting of the data for QC release from Zn/Al-LDH-QC composite into sodium sulphate solution for the (a) zero order, (b) first-order, (c) pseudo second order, (d) parabolic diffusion, and (e) Fickian diffusion models.

deduced that the accumulated release was found to be higher whenever PO_4^{3-} anions were present in the release media. This therefore demonstrates that the presence of PO_4^{3-} anions in release media greatly influence the accumulated release of QC and the rate of the release process, thus dominating the whole release process.

3.7. Kinetic study of Zn/Al-LDH-QC composite release into various aqueous solution

An attempt has been made to fit the result obtained from the release study of Zn/Al-LDH-QC to several kinetic models, to gain some insight into the release kinetics. The profiles of Zn/Al-LDH-QC composite release into aqueous solutions of Na_3PO_4, Na_2SO_4 and NaCl are shown in Figs. 8–10, respectively. Five different models were selected to be used in the study, including zero order (Equation (i)), first-order (Equation (ii)) [56], pseudo second order (Equation (iii)) [57], parabolic diffusion (Equation (iv)) [58] and Fickian diffusion (Equation (v)) [59] models. The equations of each kinetic model are provided below, where x represents the percentage release of QC from the interlayer gallery of Zn/Al-LDH at time t, c refers to a constant, M_i is the initial concentration of QC, and M_f is the final concentration of QC.

$$x = t + c \quad \text{(i)}$$

$$-\log(1 - M_i/M_f) = t + c \quad \text{(ii)}$$

$$t/M_i = 1/M_f^2 + t/Mf \quad \text{(iii)}$$

$$M_i/M_f = kt^{0.5} + c \quad \text{(iv)}$$

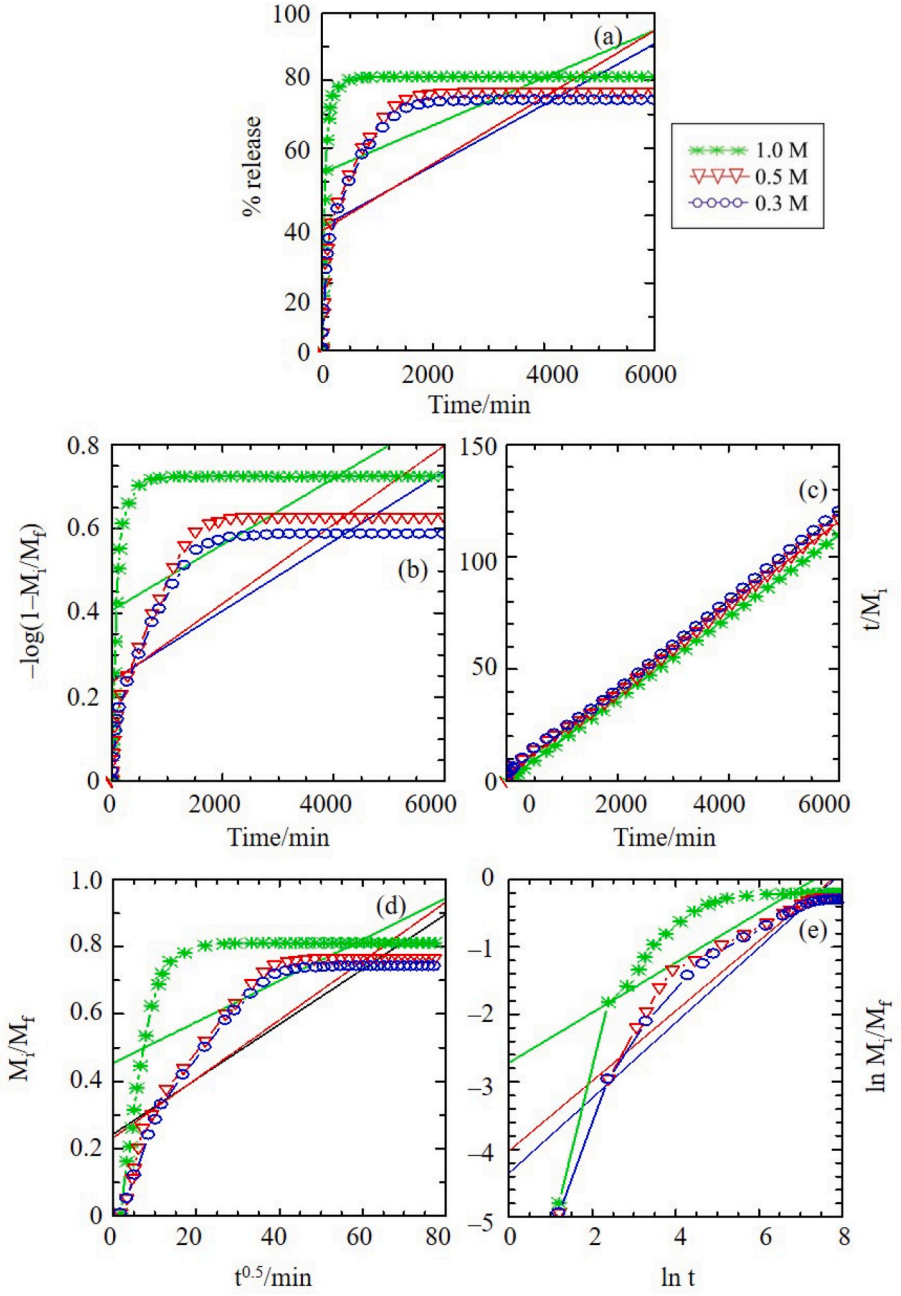

Fig. 10. Fitting of the data for QC release from Zn/Al-LDH-QC composite into sodium chloride solution for the (a) zero order, (b) first-order, (c) pseudo second order, (d) parabolic diffusion and (e) Fickian diffusion models.

Table 2
Comparison of rate constants (k), regression values (r^2) and half-life ($t_{1/2}$) obtained from the fitting of the release data from Zn/Al–LDH–QC into aqueous solutions of Na_3PO_4, Na_2SO_4 and NaCl.

Aqueous solution		Zero order	First order	Parabolic diffusion	Fickian diffusion	Pseudo-second order		
		r^2	r^2	r^2	r^2	r^2	k ($x10^{-3}s^{-1}$)	$t_{1/2}$
Na_3PO_4	0.3 M	0.524	0.605	0.786	0.995	0.999	0.135	110.0
	0.5 M	0.344	0.428	0.573	0.948	0.999	0.412	36.1
	1.0 M	0.286	0.342	0.473	0.751	0.999	1.229	12.1
Na_2SO_4	0.3 M	0.766	0.831	0.943	0.841	0.996	0.081	184.0
	0.5 M	0.446	0.544	0.704	0.850	0.998	0.216	68.8
	1.0 M	0.153	0.181	0.294	0.450	0.999	2.917	5.1
NaCl	0.3 M	0.543	0.624	0.757	0.876	0.999	0.024	622.6
	0.5 M	0.567	0.642	0.779	0.846	0.999	0.024	622.4
	1.0 M	0.346	0.419	0.517	0.585	0.999	0.175	85.0

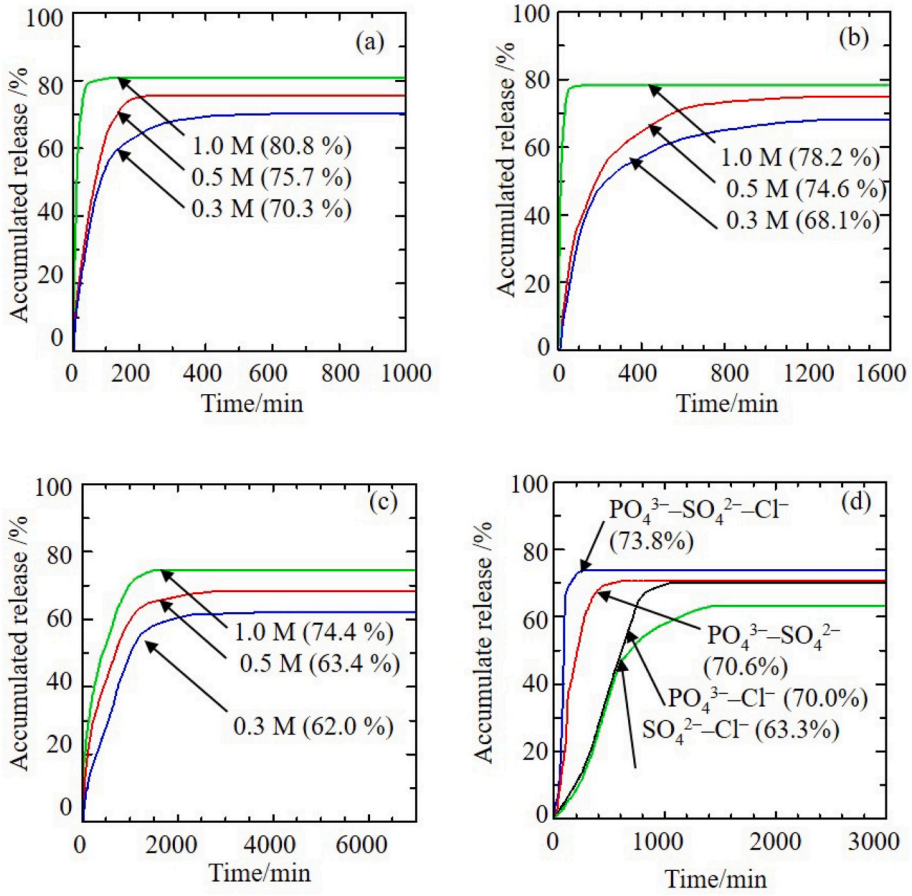

Fig. 11. Release profiles of QC from Zn/Al–LDH–QC–Chi into aqueous solutions of (a) sodium phosphate, (b) sodium sulphate, (c) sodium chloride and (d) phosphate, sulphate and chloride mixture.

Table 3
Comparison of the percentage release of QC from Zn/Al–LDH–QC and Zn/Al–LDH–QC–Chi into single, binary and ternary aqueous systems of phosphate, sulphate and chloride.

Aqueous solutions			Zn/Al–LDH–QC		Zn/Al–LDH–QC-Chi	
			Percentage release (%)	Release time (min)	Percentage release (%)	Release time (min)
Single	PO_4^{3-}	0.3 M	73.9	356	70.3	608
		0.5 M	80.5	221	75.7	265
		1.0 M	81.2	99	80.8	103
	SO_4^{2-}	0.3 M	47.2	1161	68.1	1255
		0.5 M	77.0	714	74.6	1192
		1.0 M	81.8	84	78.2	112
	Cl^-	0.3 M	73.8	2639	62.0	3176
		0.5 M	76.0	2168	63.4	2855
		1.0 M	82.4	693	74.4	1646
Binary	PO_4^{3-} – SO_4^{2}		79.2	329	70.6	611
	PO_4^{3-} – Cl^-		77.5	1015	70.0	1045
	SO_4^{2} – Cl^-		75.6	1359	73.3	1436
Ternary	PO_4^{3-} – SO_4^{2}–Cl^-		80.3	138	73.8	269

$$M_i/M_f = kt^n \quad (v)$$

The zero order, first-order and pseudo second order kinetic models are beneficial in determining the variables that have an effect on the release behaviour of the composite, while the parabolic diffusion model can be applied to determine the diffusion-controlled release of the intercalated anions into the aqueous solutions [60]. The Fickian diffusion kinetic model is useful in determining the mode of kinetics based on the diffusion exponent value, n, obtained from the kinetic equation [61]. A value of $n = 0.5$ represents Fickian diffusion, which indicates that the release is diffusion-controlled (Higuchi model) and $0.5 < n < 1$ signifies anomalous diffusion, which reveals that the release occurs in both diffusion-controlled and erosion-controlled manners. A value of $n = 1$ demonstrates case II transport, with a constant release rate controlled by polymer relaxation. Lastly, a value of $n > 1$ represents super case II transport, indicating that the release is erosion controlled. The release kinetics shown by the composite is influenced by their degradation mode and rate, swelling rate, absorption limit, molecular weight, and composition.

The rate constant k was calculated based on the equations of the kinetic models where the half-time $t_{1/2}$ represents the time required to increase 50% of accumulated saturated value of BP, obtained from the release profile. The regression values r^2 were obtained by fitting the release data to each kinetic model, and the values of r^2 closest to 1 were considered as the best fit for the release. The values of k, $t_{1/2}$ and r^2 are summarised in Table 2.

As can be seen from the release data, the plot of t/Mi against time shows good agreement with the pseudo second order kinetic model. The

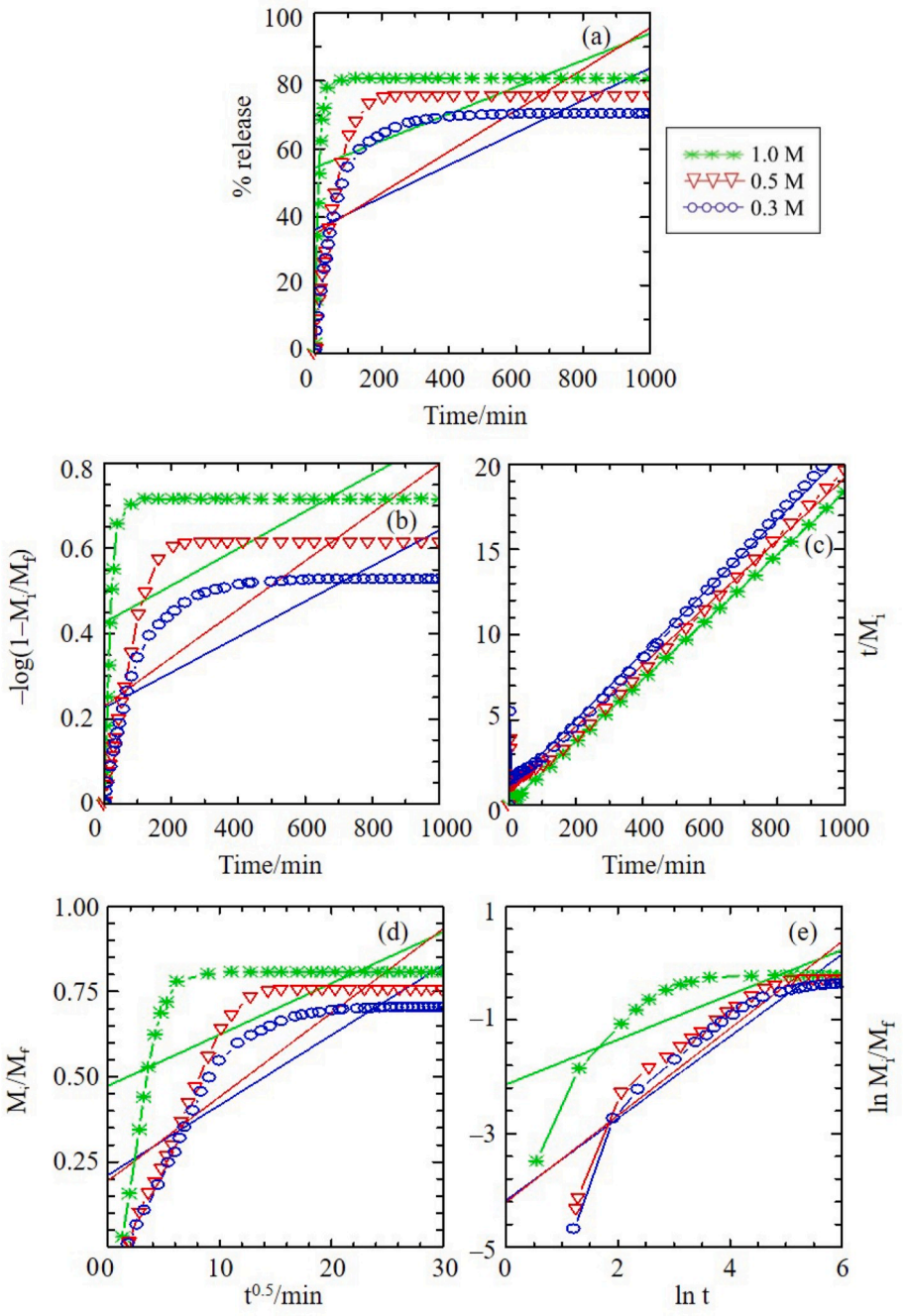

Fig. 12. Fitting of the data for QC release from Zn/Al–LDH–QC–Chi into aqueous solution of sodium phosphate for the (a) zero order, (b) first order, (c) pseudo second order, (d) parabolic diffusion and (e) Fickian diffusion kinetic models.

values of r^2 gave the best fit for the pseudo second order kinetic model, in the range of 0.996–0.999. The linearisation of other kinetic models seems to fit the data obtained from the release study poorly, with significantly low r^2 values. Hence, the pseudo second order kinetic model is more satisfactory in expressing the kinetic behaviour of release of QC from the Zn/Al-LDH-QC composite. The kinetic behaviour shown by the composite indicates that the release process occurs via dissolution of the composite and ion exchange between the intercalated QC and the anions available in the release media [62]. The release profile also reveals that most of the release of the intercalated QC takes place in the early part of the release process, before release equilibrium is achieved. This release trend is known as 'burst release', which happens because of the swelling of the porous structure of the composite and the dissolution of the intercalated anions. The burst release takes place in a very short time compared to the total duration of the release process; hence causing a slight deviation from the linearity of the pseudo second order curve fit at the start of the release process [63].

The $t_{1/2}$ values of the release data generally show that the presence of PO_4^{3-} in the release media increases the rate of the release process, with lowest $t_{1/2}$ values, followed by SO_4^{2-} and Cl^-. This shows that the charge density of the anions in the release media has an effect on the $t_{1/2}$ values of the release process. It is also noticeable from the release data that increasing the concentration of the aqueous solution results in a reduction of the $t_{1/2}$ values; hence demonstrating that the process of release of the intercalated QC into aqueous solution occurs more readily into aqueous solutions of higher concentration, as more ions are present [62].

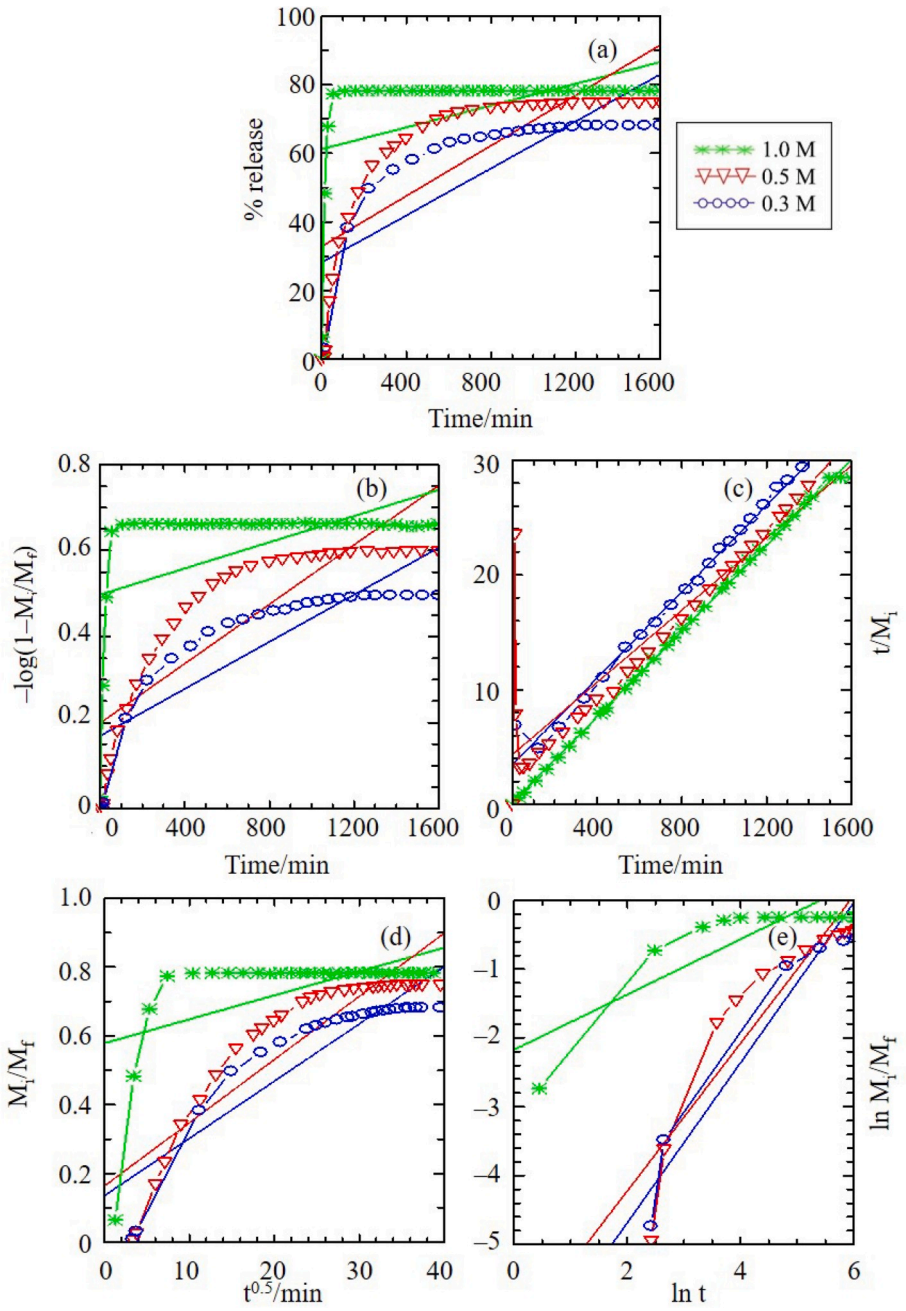

Fig. 13. Fitting of the data for QC release from Zn/Al–LDH–QC–Chi into aqueous solution of sodium sulphate for the (a) zero order, (b) first order, (c) pseudo second order, (d) parabolic diffusion and (e) Fickian diffusion kinetic models.

3.8. Study of release from Zn/Al-LDH-QC-Chi composite into various aqueous solutions

The release study of QC from the Zn/Al–LDH–QC–Chi composite was also conducted in single, binary and ternary system of aqueous solutions of Na_3PO_4, Na_2SO_4 and NaCl, using the same set of concentrations as in the study of release from Zn/Al–LDH–QC. Similar experimental conditions of UV–vis measurements were also applied throughout the release study of the Zn/Al-LDH-QC-Chi composite, so that the effect of chitosan coating on the release of the intercalated QC could be observed properly. The release profiles of QC from Zn/Al-LDH-QC-Chi composite into the aqueous solution of Na_3PO_4, Na_2SO_4 and NaCl are shown in Fig. 11.

Based on the release profile, it can be seen that the highest accumulated release is achieved when the Zn/Al-LDH-QC-Chi composite releases into the aqueous solution of Na_3PO_4, with 68.1, 74.6 and 78.2% release for 0.3 M, 0.5 M and 1.0 M Na_3PO_4, respectively. The percentage release decreased when Na_2SO_4 aqueous solution was used as the release medium and seems to decrease continuously when the Zn/Al-LDH-QC-Chi composite releases into the aqueous solution of NaCl. The lowest accumulated release of 62.0% was observed when the Zn/Al-LDH-QC-Chi released into 0.3 M NaCl aqueous solution. Increasing the concentration of the aqueous solution also resulted in the Zn/Al-LDH-QC-Chi composite achieving greater percentage release. Even though the release trend seems to be the same as in the release study of Zn/Al-LDH-QC, a significant delay in the time taken for the release of intercalated QC to reach equilibrium is noticeable in the release profile of the Zn/Al-LDH-QC-Chi composite.

The release profile obtained revealed that the release of the Zn/Al-LDH-QC-Chi composite in binary and ternary systems of aqueous solutions shared a similar trend as in the release of the Zn/Al-LDH-QC

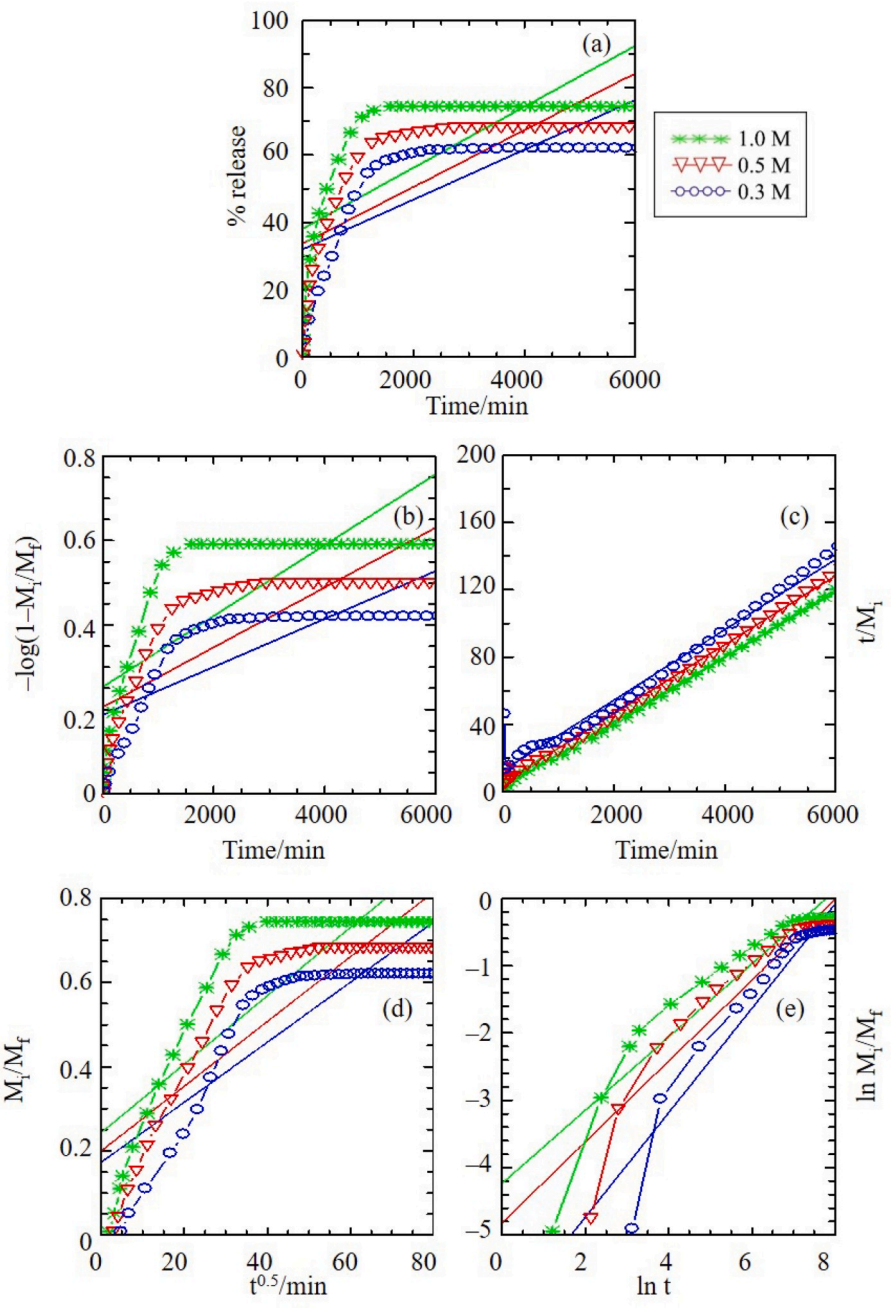

Fig. 14. Fitting of the data for QC release from Zn/Al–LDH–QC–Chi into aqueous solution of sodium chloride for the (a) zero order, (b) first order, (c) pseudo second order, (d) parabolic diffusion and (e) Fickian diffusion kinetic models.

Table 4
Comparison of rate constants (k), regression values (r^2) and half-life ($t_{1/2}$) obtained from the fitting of the release data from Zn/Al–LDH–QC–Chi into aqueous solutions of Na_3PO_4, Na_2SO_4 and NaCl.

Aqueous solution		Zero order	First order	Parabolic diffusion	Fickian diffusion	Pseudo-second order		
		r^2	r^2	r^2	r^2	r^2	k ($x10^{-3}s^{-1}$)	$t_{1/2}$
Na_3PO_4	0.3 M	0.542	0.625	0.758	0.841	0.986	0.135	110.0
	0.5 M	0.518	0.584	0.735	0.851	0.985	0.412	36.1
	1.0 M	0.300	0.375	0.463	0.610	0.999	1.229	12.1
Na_2SO_4	0.3 M	0.616	0.717	0.809	0.943	0.988	0.081	184.0
	0.5 M	0.609	0.727	0.812	0.844	0.999	0.216	68.8
	1.0 M	0.196	0.223	0.301	0.721	0.778	2.917	5.1
NaCl	0.3 M	0.532	0.588	0.725	0.909	0.969	0.024	622.6
	0.5 M	0.568	0.633	0.765	0.890	0.997	0.024	622.4
	1.0 M	0.528	0.997	0.734	0.875	0.999	0.175	85.0

composite. The highest percentage of accumulated release was obtained when the aqueous solution containing PO_4^{3-}, SO_4^{2-} and Cl^- was used as the release medium. A total of 73.8% of intercalated QC was released from the interlayer gallery of the Zn/Al-LDH-QC-Chi composite in 269 min. The second highest percentage of accumulated release was obtained when the release study was carried out in an aqueous solution containing PO_4^{3-} and SO_4^{2-} anions with 70.6% of accumulated release within 611 min, which was then followed by the release in aqueous solutions of PO_4^3 and Cl^- (70.0%), and SO_4^{2-} and Cl^- (63.3%), with time releases of 1045 and 1436 min, respectively. Although the trends in the release behaviour of the Zn/Al-LDH-QC and Zn/Al-LDH-QC-Chi composites are quite similar, the time releases of QC from the Zn/Al-LDH-QC-Chi composite are longer than those observed in the release profile of the Zn/Al-LDH-QC composite. This therefore validates the potential of chitosan coating in extending the time release of QC. The comparison between the accumulated percentage release and the time taken for the release of QC from the Zn/Al-LDH-QC and Zn/Al-LDH-QC-Chi composites to reach equilibrium in each aqueous solution is shown in Table 3.

The polycationic properties of the chitosan play an important part in slowing the release rate of Zn/Al-LDH-QC-Chi. The positively charged amino group on the backbone of the chitosan can form electrostatic interactions with the negatively charged QC anion, and hence strengthen the electrostatic attractions that formerly existed between the QC anions and the Zn/Al-LDH layers. The stronger electrostatic attractions formed result in the QC anions being held more tightly in the interlayer gallery of the Zn/Al-LDH-QC composite, thus increasing the time taken for the ion exchange process to occur between the QC anions and the anions in the release medium. The impact of polycationic properties of chitosan in slowing the release of intercalated guest ion is in good agreement with previous studies [43,64,65]. Although the polycationic properties of chitosan also generally caused the percentage release to decrease, the reduction was not too significant as the percentage release was only slightly changed. The positive impact of chitosan on the controlled release behaviour of Zn/Al-LDH therefore shows good agreement with many recent studies [21,45,66,67].

3.9. Kinetic study of release from Zn/Al-LDH-QC-Chi composite into various aqueous solutions

The kinetic study of Zn/Al-LDH-QC-Chi was also evaluated using zero order, first-order, pseudo second order, parabolic diffusion and Fickian diffusion models, similar to the kinetic study of Zn/Al-LDH-QC. Fitting of the data for QC release from the Zn/Al-LDH-QC-Chi composite into each kinetic model is shown in Figs. 12–14. The values of k, $t_{1/2}$ and r^2 are summarised in Table 4.

Based on the data fitting and the table constructed, it can be observed that the value of r^2 for each release is closest to 1 when fitted to the pseudo second order model ($r^2 \geq 0.778$). The $t_{1/2}$ values generally decreased in the order $Cl^- > SO_4^{2-} > PO_4^{3-}$. The occurrence of the 'burst release' phenomena due to the release of large numbers of QC anions at the beginning of the release may also be observed in each release data. The results from the kinetic study of Zn/Al-LDH-QC-Chi therefore demonstrate a comparable pattern of release behaviour to that shown by both Zn/Al-LDH-QC and Zn/Al-LDH-QC-Chi composites. Similar to the Zn/Al-LDH-QC composite, the release of the intercalated QC from Zn/Al-LDH-QC-Chi also took place via dissolution and ion exchange. Thus, based on the kinetic study conducted, it was revealed that the coating process did not causing any alteration in the release mechanism of the composite.

4. Conclusion

The results obtained from the characterisation studies prove that the Zn/Al-LDH-QC composite can successfully be coated using chitosan without interfering in the intercalation of QC in the interlayer gallery of Zn/Al-LDH. In fact, TGA/DTG also demonstrated that the chitosan coating does improve the thermal stabilities of the synthesised composite. A comparison of the release studies has been made based on the release behaviour of both Zn/Al-LDH-QC and Zn/Al-LDH-QC-Chi. The results from the release studies show that the Zn/Al-LDH itself is an effective inorganic matrix to sustain the release of QC to the release medium. However, when Zn/Al-LDH-QC undergoes the coating process, the presence of chitosan on the outer surface of the Zn/Al-LDH-QC seems to strengthen the electrostatic attraction between the QC anions and the amine groups on the chitosan, thus helping to enhance the controlled release behaviour of the composite. The results obtained show that both composites follow pseudo second order models, hence show the same release mechanism. In summary, the results suggest that the use of Zn/Al-LDH as host material with chitosan coating may be useful in retarding the release of QC herbicide after soil application in paddy cultivation areas, hence avoiding the environmental problems that might arise from the rapid leaching through the soil profile.

Declaration of competing interest

The authors declare that they have no known competing financial interests or personal relationships that could have appeared to influence the work reported in this paper.

Acknowledgement

The authors wish to thank UPSI and Ministry of Education Malaysia for the support during completing the research. This work was supported by the GPU-RISING STAR Grant No. 2019−0119−103−01.

Appendix A. Supplementary data

Supplementary data to this article can be found online at https://doi.org/10.1016/j.matchemphys.2020.123076.

References

[1] H. Azejjel, C. Del Hoyo, K. Draoui, M.S. Rodríguez-Cruz, M.J. Sánchez-Martín, Natural and modified clays from Morocco as sorbents of ionizable herbicides in aqueous medium, Desalination 249 (2009) 1151–1158, https://doi.org/10.1016/j.desal.2009.02.066.
[2] A.A. Masoud, N.A. Abdel-Wahab Arafa, M. El-Bouraie, Patterns and trends of the pesticide pollution of the shallow nile delta aquifer (Egypt), water, Air. Soil Pollut. 229 (2018), https://doi.org/10.1007/s11270-018-3802-5.
[3] M.S. Sankhla, Water contamination through pesticide & their toxic effect on human health, Int. J. Res. Appl. Sci. Eng. Technol. 6 (2018) 967–970, https://doi.org/10.22214/ijraset.2018.1146.
[4] E. Carazo-Rojas, G. Pérez-Rojas, M. Pérez-Villanueva, C. Chinchilla-Soto, J.S. Chin-Pampillo, P. Aguilar-Mora, M. Alpízar-Marín, M. Masís-Mora, C.E. Rodríguez-Rodríguez, Z. Vryzas, Pesticide monitoring and ecotoxicological risk assessment in surface water bodies and sediments of a tropical agro-ecosystem, Environ. Pollut. 241 (2018) 800–809, https://doi.org/10.1016/j.envpol.2018.06.020.
[5] A. Diendéré, G. Nguyen, J.P. Del Corso, C. Kephaliacos, Modeling the relationship between pesticide use and farmers' beliefs about water pollution in Burkina Faso, Ecol. Econ. 151 (2018) 114–121, https://doi.org/10.1016/j.ecolecon.2018.05.002.
[6] S. Jin, B. Bluemling, A.P.J. Mol, Mitigating land pollution through pesticide packages – the case of a collection scheme in Rural China, Sci. Total Environ. 622–623 (2018) 502–509, https://doi.org/10.1016/j.scitotenv.2017.11.330.
[7] R.M. Toichuev, L.V. Zhilova, G.B. Makambaeva, T.R. Payzildaev, W. Pronk, M. Bouwknegt, R. Weber, Assessment and review of organochlorine pesticide pollution in Kyrgyzstan, Environ. Sci. Pollut. Res. 25 (2018) 31836–31847, https://doi.org/10.1007/s11356-017-0001-7.
[8] M. Solé, M. Bonsignore, G. Rivera-Ingraham, R. Freitas, Exploring alternative biomarkers of pesticide pollution in clams, Mar. Pollut. Bull. 136 (2018) 61–67, https://doi.org/10.1016/j.marpolbul.2018.08.062.
[9] T. Bashnin, V. Verhaert, M. De Jonge, L. Vanhaecke, J. Teuchies, L. Bervoets, Relationship between pesticide accumulation in transplanted zebra mussel (Dreissena polymorpha) and community structure of aquatic macroinvertebrates, Environ. Pollut. 252 (2019) 591–598, https://doi.org/10.1016/j.envpol.2019.05.140.
[10] T. Mhadhbi, O. Pringault, H. Nouri, S. Spinelli, H. Beyrem, C. Gonzalez, Evaluating polar pesticide pollution with a combined approach: a survey of agricultural

practices and POCIS passive samplers in a Tunisian lagoon watershed, Environ. Sci. Pollut. Res. 26 (2019) 342–361, https://doi.org/10.1007/s11356-018-3552-3.
[11] T. Skevas, Evaluating alternative policies to reduce pesticide groundwater pollution in Dutch arable farming, J. Environ. Plann. Manag. (2019) 1–18, https://doi.org/10.1080/09640568.2019.1606618, 0.
[12] R. Grillo, N.Z.P. Dos Santos, C.R. Maruyama, A.H. Rosa, R. De Lima, L.F. Fraceto, Poly(ε-caprolactone)nanocapsules as carrier systems for herbicides: physico-chemical characterization and genotoxicity evaluation, J. Hazard Mater. 231–232 (2012) 1–9, https://doi.org/10.1016/j.jhazmat.2012.06.019.
[13] S.A. Seven, Ö.F. Tastan, C.E. Tas, H. Ünal, İ.A. Ince, Y.Z. Menceloglu, Insecticide-releasing LLDPE films as greenhouse cover materials, Mater. Today Commun. 19 (2019) 170–176, https://doi.org/10.1016/j.mtcomm.2019.01.015.
[14] T.A. Wani, F.A. Masoodi, W.N. Baba, M. Ahmad, N. Rahmanian, S.M. Jafari, Nanoencapsulation of Agrochemicals, Fertilizers, and Pesticides for Improved Plant Production, Elsevier Inc., 2019, https://doi.org/10.1016/b978-0-12-815322-2.00012-2.
[15] L. Cao, Y. Liu, C. Xu, Z. Zhou, P. Zhao, S. Niu, Q. Huang, Biodegradable poly(3-hydroxybutyrate-co-4-hydroxybutyrate) microcapsules for controlled release of trifluralin with improved photostability and herbicidal activity, Mater. Sci. Eng. C 102 (2019) 134–141, https://doi.org/10.1016/j.msec.2019.04.050.
[16] C. Tang, Y. Li, J. Pun, A.S. Mohamed Osman, K.C. Tam, Polydopamine microcapsules from cellulose nanocrystal stabilized Pickering emulsions for essential oil and pesticide encapsulation, Colloids Surfaces A Physicochem. Eng. Asp. 570 (2019) 403–413, https://doi.org/10.1016/j.colsurfa.2019.03.049.
[17] Q. Xu, G. Liu, Y. Zhou, F. Nie, Preparation and properties of photo-responsive controlled release pesticide film, Adv. Eng. Res. 181 (2019) 230–233, https://doi.org/10.2991/ice2me-19.2019.53.
[18] M.C. Neri-Badang, S. Chakraborty, Carbohydrate polymers as controlled release devices for pesticides, J. Carbohydr. Chem. 38 (2019) 67–85, https://doi.org/10.1080/07328303.2019.1568449.
[19] S.N.M. Sharif, N. Hashim, I.M. Isa, M.I. Saidin, M.S. Ahmad, M. Mamat, M. Z. Hussein, Controlled release formulation of zinc hydroxide nitrate intercalated with sodium dodecylsulphate and bispyribac Anions : a novel herbicide nanocomposite for paddy cultivation, Arab. J. Chem. (2019), https://doi.org/10.1016/j.arabjc.2019.09.006.
[20] B. Azeem, K. Kushaari, Z.B. Man, A. Basit, T.H. Thanh, Review on materials & methods to produce controlled release coated urea fertilizer, J. Contr. Release 181 (2014) 11–21, https://doi.org/10.1016/j.jconrel.2014.02.020.
[21] D. Davidson, F.X. Gu, Materials for sustained and controlled release of nutrients and molecules to support plant growth, J. Agric. Food Chem. 60 (2012) 870–876, https://doi.org/10.1021/jf204092h.
[22] E. Corradini, M.R. De Moura, L.H.C. Mattoso, A preliminary study of the incorporation of NPK fertilizer into chitosan nanoparticles, Express Polym. Lett. 4 (2010) 509–515, https://doi.org/10.3144/expresspolymlett.2010.64.
[23] H. Dong, F. Li, J. Li, Y. Li, Characterizations of blend gels of carboxymethylated polysaccharides and their use for the controlled release of herbicide, J. Macromol. Sci. Part A Pure Appl. Chem. 49 (2012) 235–241, https://doi.org/10.1080/10601325.2012.649204.
[24] M.Z. Hussein, Z. Zainal, A.H. Yahaya, D.W.V. Foo, Controlled release of a plant growth regulator, alpha-naphthaleneacetate from the lamella of Zn-Al-layered double hydroxide nanocomposite, J. Contr. Release 82 (2002) 417–427, doi: S0168365902001724 [pii].
[25] D. Legras-Lecarpentier, K. Stadler, R. Weiss, G.M. Guebitz, G.S. Nyanhongo, Enzymatic synthesis of 100% lignin biobased granules as fertilizer storage and controlled slow release systems, ACS Sustain. Chem. Eng. 7 (2019) 12621–12628, https://doi.org/10.1021/acssuschemeng.9b02689.
[26] S. Bakhtiary, M. Shirvani, H. Shariatmadari, Adsorption-desorption behavior of 2,4-D on NCP-modified bentonite and zeolite: implications for slow-release herbicide formulations, Chemosphere 90 (2013) 699–705, https://doi.org/10.1016/j.chemosphere.2012.09.052.
[27] J. Garrido, F. Cagide, M. Melle-Franco, F. Borges, E.M. Garrido, Microencapsulation of herbicide MCPA with native β-cyclodextrin and its methyl and hydroxypropyl derivatives: an experimental and theoretical investigation, J. Mol. Struct. 1061 (2014) 76–81, https://doi.org/10.1016/j.molstruc.2013.12.067.
[28] Z. Fang, B. Bhandari, Encapsulation of polyphenols–a review, Trends Food Sci. Technol. 21 (2010) 510–523.
[29] V. Nedovic, A. Kalusevic, V. Manojlovic, S. Levic, B. Bugarski, An overview of encapsulation technologies for food applications, Procedia Food Sci 1 (2011) 1806–1815, https://doi.org/10.1016/j.profoo.2011.09.265.
[30] D.H. Park, S.J. Hwang, J.M. Oh, J.H. Yang, J.H. Choy, Polymer-inorganic supramolecular nanohybrids for red, white, green, and blue applications, Prog. Polym. Sci. 38 (2013) 1442–1486, https://doi.org/10.1016/j.progpolymsci.2013.05.007.
[31] W. Pon-On, T. Tithito, W. Maneeprakorn, T. Phenrat, I.M. Tang, Investigation of magnetic silica with thermoresponsive chitosan coating for drug controlled release and magnetic hyperthermia application, Mater. Sci. Eng. C 97 (2019) 23–30, https://doi.org/10.1016/j.msec.2018.11.076.
[32] M. Criado-Gonzalez, M. Fernandez-Gutierrez, J. San Roman, C. Mijangos, R. Hernández, Local and controlled release of tamoxifen from multi (layer-by-layer) alginate/chitosan complex systems, Carbohydr. Polym. 206 (2019) 428–434, https://doi.org/10.1016/j.carbpol.2018.11.007.
[33] S. Song, Y. Wang, J. Xie, B. Sun, N. Zhou, H. Shen, J. Shen, Carboxymethyl chitosan modified carbon nanoparticle for controlled emamectin benzoate delivery: improved solubility, pH-responsive release, and sustainable pest control, ACS Appl. Mater. Interfaces (2019), https://doi.org/10.1021/acsami.9b12564.
[34] S.Z. Md Rasib, H. Md Akil, A. Khan, Z.A. Abdul Hamid, Controlled release studies through chitosan-based hydrogel synthesized at different polymerization stages, Int. J. Biol. Macromol. 128 (2019) 531–536, https://doi.org/10.1016/j.ijbiomac.2019.01.190.
[35] S. Xu, H. Li, H. Ding, Z. Fan, P. Pi, J. Cheng, X. Wen, Allylated chitosan-poly(N-isopropylacrylamide) hydrogel based on a functionalized double network for controlled drug release, Carbohydr. Polym. 214 (2019) 8–14, https://doi.org/10.1016/j.carbpol.2019.03.008.
[36] S.T. Khalili, A. Mohsenifar, M. Beyki, S. Zhaveh, T. Rahmani-Cherati, A. Abdollahi, M. Bayat, M. Tabatabaei, Encapsulation of Thyme essential oils in chitosan-benzoic acid nanogel with enhanced antimicrobial activity against Aspergillus flavus, LWT - Food Sci. Technol. (Lebensmittel-Wissenschaft -Technol.) 60 (2015) 502–508.
[37] M.A. Azevedo, A.I. Bourbon, A.A. Vicente, M.A. Cerqueira, Alginate/chitosan nanoparticles for encapsulation and controlled release of vitamin B2, Int. J. Biol. Macromol. 71 (2014) 141–146, https://doi.org/10.1016/j.ijbiomac.2014.05.036.
[38] N.M. Alves, J.F. Mano, Chitosan derivatives obtained by chemical modifications for biomedical and environmental applications, Int. J. Biol. Macromol. 43 (2008) 401–414.
[39] F. Donsì, M. Annunziata, M. Sessa, G. Ferrari, Nanoencapsulation of essential oils to enhance their antimicrobial activity in foods, LWT - Food Sci. Technol. (Lebensmittel-Wissenschaft -Technol.) 44 (2011) 1908–1914.
[40] S.N.M. Sharif, N. Hashim, I. Md Isa, N.M. Ali, S.A. Bakar, M.Z. Hussein, M. Mamat, N.A. Bakar, W.R.W. Mahamod, Preparation and characterisation of novel paddy cultivation herbicide nanocomposite from zinc/aluminium layered double hydroxide and quinclorac anion, Mater. Res. Innovat. (2018), https://doi.org/10.1080/14328917.2018.1452586, 10.1080/14328917.2018.1452586.
[41] L. Zhan, Y. Du, Z. Zhang, D. Pang, Preparation and characterization of CdS quantum dots chitosan biocomposite, React. Funct. Polym. 55 (2003) 35–43, https://doi.org/10.1016/S1381-5148(02)00197-9.
[42] S.H. Sarijo, S.A.I.S.M. Ghazali, M.Z. Hussein, A.H. Ahmad, Intercalation, physicochemical and controlled release studies of organic-inorganic–herbicide (2,4,5 tricholorphenoxy butyric acid) nanohybrid into hydrotalcite-like compounds, Mater. Today Proc. 2 (2015) 345–354, https://doi.org/10.1016/j.matpr.2015.04.061.
[43] C. Sanjai, S. Kothan, P. Gonil, S. Saesoo, W. Sajomsang, Chitosan-triphosphate nanoparticles for encapsulation of super-paramagnetic iron oxide as an MRI contrast agent, Carbohydr. Polym. 104 (2014) 231–237, https://doi.org/10.1016/j.carbpol.2014.01.012.
[44] Y. Luo, Z. Teng, Y. Li, Q. Wang, Solid lipid nanoparticles for oral drug delivery: chitosan coating improves stability, controlled delivery, mucoadhesion and cellular uptake, Carbohydr. Polym. 122 (2015) 221–229, https://doi.org/10.1016/j.carbpol.2014.12.084.
[45] S.F. Hosseini, M. Zandi, M. Rezaei, F. Farahmandghavi, Two-step method for encapsulation of oregano essential oil in chitosan nanoparticles: preparation, characterization and in vitro release study, Carbohydr. Polym. 95 (2013) 50–56, https://doi.org/10.1016/j.carbpol.2013.02.031.
[46] M.Z. Hussein, Z.B. Jubri, Z. Zainal, A.H. Yahya, Pamoate intercalated Zn-Al layered double hydroxide for the formation of layered organic-inorganic intercalate, Mater. Sci. 22 (2004) 57–67.
[47] F. Barahuie, M.Z. Hussein, P. Arulselvan, S. Fakurazi, Z. Zainal, Drug delivery system for an anticancer agent, chlorogenate-Zn/Al-layered double hydroxide nanohybrid synthesised using direct co-precipitation and ion exchange methods, J. Solid State Chem. 217 (2014) 31–41, https://doi.org/10.1016/j.jssc.2014.04.015.
[48] S. Li, Y. Shen, M. Xiao, D. Liu, L. Fan, Synthesis and controlled release properties of β-naphthoxyacetic acid intercalated Mg–Al layered double hydroxides nanohybrids, Arab, J. Chem. (2015), https://doi.org/10.1016/j.arabjc.2015.04.034, 10.1016/j.arabjc.2015.04.034.
[49] J.M. Fernandez, M.A. Ulibarri, F.M. Labajos, V. Rives, The effect of iron on the crystalline phases formed upon thermal decomposition of Mg–Al–Fe hydrotalcites, J. Mater. Chem. 8 (1998) 2507–2514.
[50] N. Hashim, M.Z. Hussein, I.M. Isa, A. Kamari, A. Mohamed, Layered double hydroxide as a potential matrix for controlled release formulation for phenoxyherbicide, J. Sains Dan Mat. 4 (2012) 22–36.
[51] S.H. Sarijo, S.A.I.S.M. Ghazali, M.Z. Hussein, N.J. Sidek, Synthesis of nanocomposite 2-methyl-4-chlorophenoxyacetic acid with layered double hydroxide: physicochemical characterization and controlled release properties, J. Nanoparticle Res. 15 (2013) 1–9, https://doi.org/10.1007/s11051-012-1356-9.
[52] M.Z. Hussein, N. Hashim, A. Yahaya, Z. Zainal, Synthesis of dichlorprop-Zn/Al-hydrotalcite nanohybrid and its controlled release property, Sains Malays. 40 (2011) 887–896.
[53] A.M. Bashi, M.Z. Hussein, Z. Zainal, M. Rahmani, D. Tichit, Simultaneous intercalation and release of 2,4-dichloro- and 4-chloro-phenoxy acetates into Zn/Al layered double hydroxide, Arab, J. Chem. 9 (2016) 1457–1463, https://doi.org/10.1016/j.arabjc.2012.03.015.
[54] S.A.I.S.M. Ghazali, M.Z. Hussein, S.H. Sarijo, 3,4-Dichlorophenoxyacetate interleaved into anionic clay for controlled release formulation of a new environmentally friendly agrochemical, Nanoscale Res. Lett. 8 (2013) 1–8, https://doi.org/10.1186/1556-276X-8-362.
[55] M.Z. Hussein, N. Hashim, A.H. Yahaya, Z. Zainal, Controlled release formulation of agrochemical pesticide based on 4-(2,4-dichlorophenoxy)butyrate nanohybrid, J. Nanosci. Nanotechnol. 9 (2009) 2140–2147.
[56] M.Z. Hussein, N.S.S.A. Rahman, S.H. Sarijo, Z. Zainal, Synthesis of a monophasic nanohybrid for a controlled release formulation of two active agents simultaneously, Appl. Clay Sci. 58 (2012) 60–66, https://doi.org/10.1016/j.clay.2012.01.012.

[57] Y.S. Ho, G. Mckay, Pseudo-second order model for sorption processes, Process Biochem. 34 (1999) 451–465.
[58] T. Kodama, Y. Harada, M. Ueda, K.I. Shimizu, K. Shuto, S. Komarneni, Selective exchange and fixation of strontium ions with ultrafine Na-4-mica, Langmuir 17 (2001) 4881–4886, https://doi.org/10.1021/la001774w.
[59] P.L. Ritger, N.A. Peppas, A simple equation for description of solute release II. Fickian and anomalous release from swellable devices, J. Contr. Release 5 (1987) 37–42.
[60] A.F. Abdul Latip, M.Z. Hussein, J. Stanslas, C.C. Wong, R. Adnan, A.F.A. Latip, M. Z. Hussein, J. Stanslas, C.C. Wong, R. Adnan, A.F. Abdul Latip, M.Z. Hussein, J. Stanslas, C.C. Wong, R. Adnan, A.F.A. Latip, M.Z. Hussein, J. Stanslas, C. C. Wong, R. Adnan, Release behavior and toxicity profiles towards A549 cell lines of ciprofloxacin from its layered zinc hydroxide intercalation compound, Chem. Cent. J. 7 (2013) 1–11, https://doi.org/10.1186/1752-153X-7-119.
[61] E.P. Holowka, S.K. Bhatia, Drug Delivery: Materials Design and Clinical Perspective, Springer, New York, 2014.
[62] N. Hashim, Z. Muda, S.A. Hamid, I.M. Isa, A. Kamari, A. Mohamed, M.Z. Hussein, S.A. Ghani, Characterization and controlled release formulation of agrochemical herbicides based on zinc-layered hydroxide-3-(4-methoxyphenyl) propionate nanocomposite, J. Phys. Chem. Sci. 1 (2014) 1–6.
[63] M.Z. Hussein, N.S.S.A. Rahman, S.H. Sarijo, Z. Zainal, Herbicide-intercalated zinc layered hydroxide nanohybrid for a dual-guest controlled release formulation, Int. J. Mol. Sci. 13 (2012) 7328–7342, https://doi.org/10.3390/ijms13067328.
[64] S. Woranuch, R. Yoksan, Eugenol-loaded chitosan nanoparticles: I. Thermal stability improvement of eugenol through encapsulation, Carbohydr. Polym. 96 (2013) 578–585, https://doi.org/10.1016/j.carbpol.2012.08.117.
[65] J.D. Bumgardner, A. Des Rieux, N. Duhem, J. Dutta, P.K. Dutta, T. Furuike, C. Gao, W.O. Haggard, R. Jayakumar, J.A. Jennings, C. Jerome, M.R. Leedy, X. Liu, L. Ma, Z. Mao, H.J. Martin, R.A.A. Muzzarell, P.A. Norowski, N. Nwe, M. Prabaharan, V. Preat, H. Ragelle, K. Rinki, R. Riva, H. Tamura, Advances in Polymer Science, Springer-Verlag Berlin Heidelberg, London, 2011, https://doi.org/10.1007/978-3-642-27154-0.
[66] M. Vemmer, A.V. Patel, Review of encapsulation methods suitable for microbial biological control agents, Biol. Contr. 67 (2013) 380–389, https://doi.org/10.1016/j.biocontrol.2013.09.003.
[67] I. Alemzadeh, M. Vossoughi, Controlled release of paraquat from poly vinyl alcohol hydrogel, Chem. Eng. Process 41 (2011) 707–710, https://doi.org/10.1002/app.